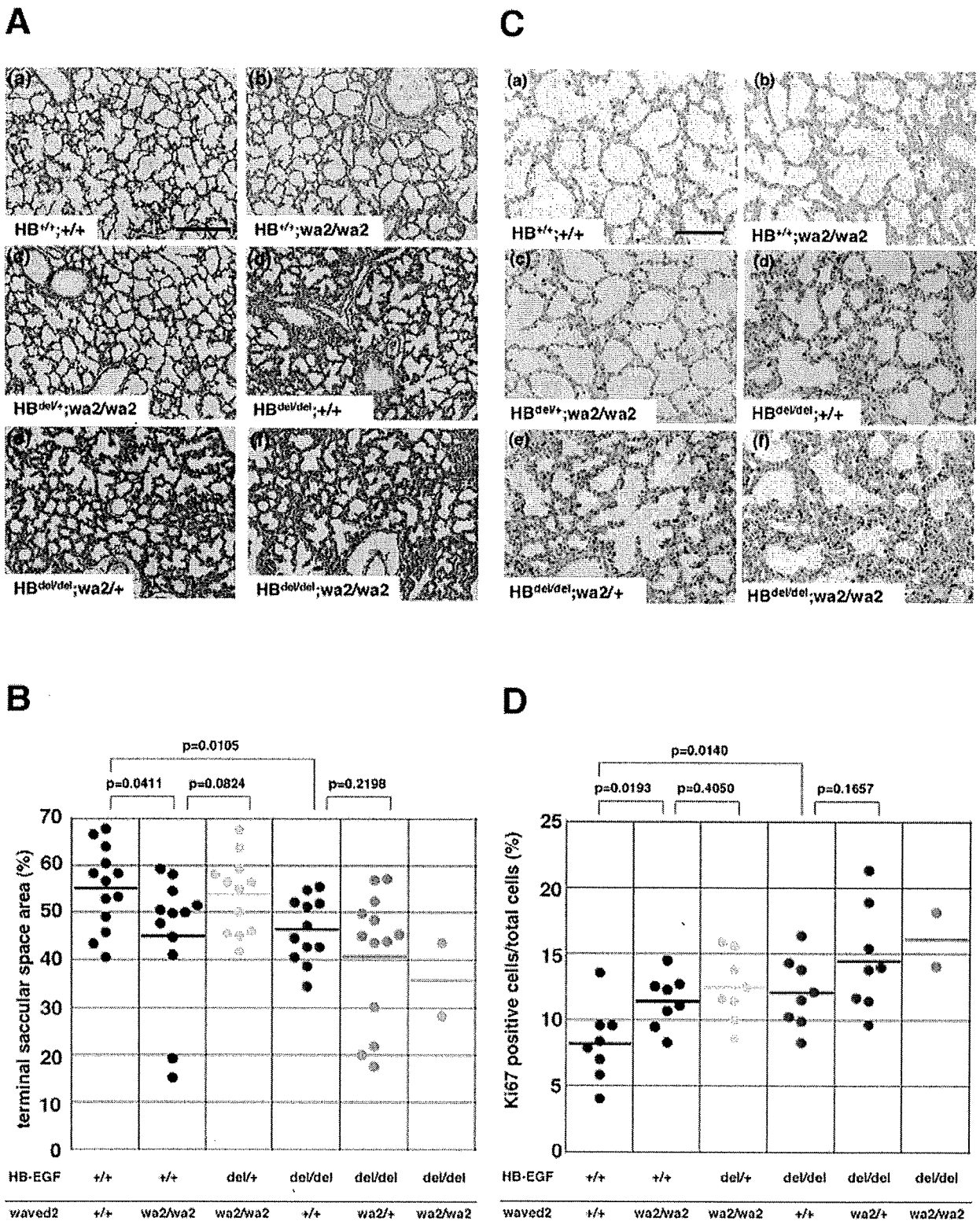
A
(a)
(b)
HB+/+;+/+
HB+/+;wa2/wa2
(c)
(d)
HBdel/+;wa2/wa2
HBdel/del;+/+
(e)
(f)
HBdel/del;wa2/+
HBdel/del;wa2/wa2
C
(a)
(b)
HB+/+;+/+
HB+/+;wa2/wa2
(c)
(d)
HBdel/+;wa2/wa2
HBdel/del;+/+
(e)
(f)
HBdel/del;wa2/+
HBdel/del;wa2/wa2
B
p=0.0105
p=0.0411
p=0.0824
p=0.2198
terminal saccular space area (%)
0
10
20
30
40
50
60
70
HB-EGF +/+ +/+ del/+ del/del del/del del/del
waved2 +/+ wa2/wa2 wa2/wa2 +/+ wa2/+ wa2/wa2
D
p=0.0140
p=0.0193
p=0.4050
p=0.1657
Ki67 positive cells/total cells (%)
0
5
10
15
20
25
HB-EGF +/+ +/+ del/+ del/del del/del del/del
waved2 +/+ wa2/wa2 wa2/wa2 +/+ wa2/+ wa2/wa2

Fig. 7.

processes of cardiac valve development and lung saccular development remain unclear. It will be interesting to investigate whether a common mechanism underlies in these two HB-EGF–mediated developmental processes.

A physiological role of TGFα in lung saccular development has remained unknown up to this study. A recent study showed that conditional transgenic mice in which TGFα was overexpressed in prenatal lung had exhibited abnormal lung morphology at birth, characterized by mesenchymal thickening, vascular remodeling, and poor apposition of capillaries to distal airspaces. Moreover, these mice died within a week after birth. In those lungs, proliferation was enhanced and the number of type II epithelial cells was increased (Kramer et al., 2007). By contrast, lung abnormalities have not been reported in TGFα null mice until now. In this study, we show that TGFα has an inhibitory function milder than HB-EGF, and TGFα functions synergistically with HB-EGF in perinatal distal lung development. There was a slight difference in quantitative comparison of TSSA, and there was an insignificant difference in the score of Ki67-positive cells between $TGF\alpha^{+/+}$ and $TGF\alpha^{-/-}$ lungs. Most of the $TGF\alpha^{-/-}$ lungs are morphologically normal, and only a few $TGF\alpha^{-/-}$ lungs exhibited abnormalities characterized by thickened saccular wall and poorly inflated sacculi. However, $HB^{del/del}$; $TGF\alpha^{+/-}$ lungs showed reduced TSSA more frequently and more cell proliferation than $HB^{del/del}$; $TGF\alpha^{+/+}$ lungs with statistical significance. To our knowledge, it is the first evidence that TGFα contributes to normal perinatal lung development. Together with the recent study of the conditional TGFα transgenic mice (Kramer et al., 2007), these results suggest that a delicate regulation of TGFα expression is important for normal lung formation in this stage. Namely, the absence of TGFα induces mild reduction of proliferation as shown in this study, while an excessive expression of TGFα in this stage also results in abnormal saccular morphology caused by hyperproliferation of the saccular cells (Kramer et al., 2007).

TGFα is expressed in bronchioles and saccular epithelia in late gestational lungs (Strandjord et al., 1993, 1994, 1995; Ruocco et al., 1996). It was reported that the expression is decreased by 50% during the transition from the canalicular (E19–E20) to the saccular (E21) stage in late-term fetal rat lung (Kubiak et al., 1992). This change of expression is consistent with our chronological analysis of TGFα mRNA expression by RT-PCR, which revealed that TGFα expression decreases in the prenatal saccular stage and rapidly increases after birth. On the other hand, HB-EGF expression is not down-regulated but rather up-regulated in the prenatal stage. This difference in expression patterns between HB-EGF and TGFα can explain the difference of phenotypic penetrance between $HB^{del/del}$ and $TGF\alpha^{-/-}$ lungs at birth. During prenatal stage, HB-EGF is expressed increasingly and mainly functions in the sacculi, while at birth, both HB-EGF and TGFα are expressed, such that in $TGF\alpha^{-/-}$ lungs, endogenous HB-EGF compensates for the lost function of TGFα during normal perinatal distal lung development.

In perinatal mouse lungs, the expression pattern of other EGFR ligands, including AR, EPR, and BTC, except for EGF, is essentially similar to TGFα. Their expressions are generally once decreased in the prenatal saccular stage. These results also suggest that HB-EGF is the primary factor among EGFR ligands responsible for normal prenatal distal lung development, and that after birth, HB-EGF may regulate cell proliferation synergistically with other EGF family ligands as well as with TGFα. It still remains unclear why the expression of other EGF family ligands except for HB-EGF initially decreases in the prenatal saccular stage during normal lung saccular development. Further study is necessary to clarify the developmental significance of those unique expression profiles and the molecular mechanisms regulating the EGFR ligands in lung saccular development during the saccular stage.

EGFR and ErbB4 are two known cognate receptors for HB-EGF (Higashiyama et al., 1991; Elenius et al., 1997). Loss of EGFR leads to an overall pulmonary malformation, including impaired branching, deficient alveolarization, reduced surfactant protein, and a marked reduction in alveolar volume in the lung (Miettinen et al., 1995; Sibilia and Wagner, 1995; Miettinen et al., 1997). These phenotypes are in part similar to that of HB-EGF null mice. Although ErbB4 null mice die at mid-gestation (E10.5) due to central nervous system and cardiac malformations (Gassmann et al., 1995), ErbB4 null mice genetically rescued from embryonic lethality by heart-specific expression of human ErbB4 are known to reach adulthood. Any lung defects has not been described in these mice (Tidcombe et al., 2003). These studies suggest that EGFR is a possible major receptor for HB-EGF at least in this process.

In this study, we genetically analyze the relationship between HB-EGF and EGFR using waved 2 mice, a hypomorphic EGFR mutant strain. Some $HB^{+/+}$; wa2/wa2 lungs exhibited a reduced TSSA and a significantly higher score in cell proliferation, compared with wild-type lungs. Moreover, $HB^{del/del}$; wa2/+ lungs exhibited a reduced TSSA more frequently and higher score of cell prolif-

Fig. 7. Comparison of TSSA and cell proliferation in double mutants of HB-EGF and waved 2 newborn pups. **A:** Representative hematoxylin/eosin-stained sections of newborn lungs from $HB^{+/+}$;+/+ (a), $HB^{+/+}$;wa2/wa2 (b), $HB^{del/+}$; wa2/wa2 (c), $HB^{del/del}$;+/+ (d), $HB^{del/del}$;wa2/+ (e), and $HB^{del/del}$;wa2/wa2 (f). **B:** Comparison of TSSA of newborn lung alveoli from $HB^{+/+}$;+/+, $HB^{+/+}$;wa2/wa2, $HB^{del/+}$;wa2/wa2, $HB^{del/del}$; +/+, $HB^{del/del}$;wa2/+, and $HB^{del/del}$;wa2/wa2. Each dot represents the percentage of TSSA from a single newborn pup, with the horizontal lines representing the mean value for each genotype (n = 12–13 in $HB^{+/+}$;+/+, $HB^{+/+}$;wa2/wa2, $HB^{del/+}$;wa2/wa2, $HB^{del/del}$;+/+ and $HB^{del/del}$;wa2/+, n = 2 in $HB^{del/del}$;wa2/wa2). **C:** Representative sections immunostained for Ki67 of newborn lung alveoli from $HB^{+/+}$;+/+ (a), $HB^{+/+}$;wa2/wa2 (b), $HB^{del/+}$;wa2/wa2 (c), $HB^{del/del}$;+/+ (d), $HB^{del/del}$;wa2/+ (e), and $HB^{del/del}$;wa2/wa2 (f). **D:** Comparison of percentage of Ki67-positive cells in total lung cells in newborn (P0) lungs from $HB^{+/+}$;+/+, $HB^{+/+}$; wa2/wa2, $HB^{del/+}$;wa2/wa2, $HB^{del/del}$;+/+, $HB^{del/del}$;wa2/+, and $HB^{del/del}$;wa2/wa2. Each dot represents the percentage of Ki67-positive cells/total cells from a single newborn pup, with the horizontal lines representing the mean value for each genotype (n = 8, in $HB^{+/+}$;+/+, $HB^{+/+}$; wa2/wa2, $HB^{del/+}$;wa2/wa2, $HB^{del/del}$;+/+ and $HB^{del/del}$;wa2/+, n = 2 in $HB^{del/del}$;wa2/wa2). For abbreviations, see list. Original magnification, ×200. Scale bar = 100 μm in A,C.

eration than $HB^{del/del}$; +/+ lungs, although without statistical significance. These results suggest that EGFR is involved in HB-EGF–mediated perinatal distal lung development. However, these results do not deny the possibilities that, as well as EGFR, other ErbB family receptors (for example, ErbB4) are also required for normal lung development. The differences in TSSA and proliferation rate between each genotype group of HB-EGF and waved 2 double-mutant mice were much less than the case of HB-EGF and TGFα double-mutant analysis. Furthermore, even waved 2 mice exhibited nearly normal lung morphology at birth and survived. Thus, it will be necessary to study the comprehensive relationship between HB-EGF and ErbB family receptors in lung development.

Almost all HB-EGF null newborns with C57BL/6J backgrounds used in this study died shortly after birth. Impaired development in $HB^{del/del}$ lungs is one possible cause of this early death of the HB-EGF null newborns. However, the penetrance of this lung phenotype is relatively low, and it was observed in only approximately half of $HB^{del/del}$ lungs, whereas the remaining $HB^{del/del}$ lungs were similar to the wild-type morphology. Although it was reported that $HB^{del/del}$ lungs showed immature lung differentiation (Jackson et al., 2003), our immunohistochemical analysis showed no remarkable change in pro-surfactant protein C expression between $HB^{+/+}$ and $HB^{del/del}$ lungs, ruling out the possibility of immature differentiation as a cause of respiratory distress. We unfortunately failed to follow the morphological change in $HB^{del/del}$ lungs after birth because of the severe perinatal lethality of HB-EGF null mice. Thus, it is possible that those lungs of $HB^{del/del}$ with apparently normal morphology rapidly deteriorate after birth, or that we do not notice other hidden severe defects than lungs in HB-EGF null mice. Despite our efforts, it still remains unclear what really causes the early death of HB-EGF null mice.

In conclusion, in the present study, we demonstrated that HB-EGF signaling contributes to perinatal distal lung development. HB-EGF functions synergistically with TGFα, and EGFR signaling regulates the decelerated cell proliferation in the perinatal distal lung. Nonetheless, the complete network of molecular mechanisms regulating these processes remains to be elucidated.

EXPERIMENTAL PROCEDURES

Mice

The generation of HB-EGF null mice ($HB^{del/del}$) has been previously described (Iwamoto et al., 2003). These mice were back-crossed for eight or nine generations onto a background of C57BL/6J strain. TGFα null and waved 2 mice were purchased from Jackson Laboratory. TGFα null mice were maintained on a background of the C57BL/6J strain. Waved 2 mice with a mixed background of C57BL/6JEi and C3H/HeSnJ when purchased, were back-crossed for four or five generations onto a background of C57BL/6J strain. For producing double-mutant mice of TGFα and HB-EGF, or waved 2 and HB-EGF, HB-EGF heterozygous or null mice that were back-crossed for three or four generations onto a background of C57/BL/6J were mated with mice described above. The finding of a vaginal plug was considered as E0.5. Timed pregnant females were killed, and embryos dissected from the uteri were placed in phosphate-buffered saline (PBS). Mice were classified as P0 when birth was witnessed and their breathing activities visualized. All mice used in this investigation were housed in Osaka University Research Institute for Microbial Diseases Animal Care Facility according to the Institutional guidelines for laboratory animals. The use and treatment of animals was approved by the Institutional Biosafety Committee on Biological Experimentation at Osaka University and the Institutional Animal Experimentation Committee at Osaka University.

Reverse Transcription PCR

Total RNA from tissues was isolated using ISOGEN (Invitrogen). One microgram of total RNA was reverse transcribed using a reverse transcriptase, ReverTra Ace (TOYOBO). PCR analysis was performed by using KOD dash (TOYOBO) for HB-EGF (98°C for 10 sec, 60°C for 2 sec, 74°C for 30 sec; 30 cycles), EGF (98°C for 10 sec, 65°C for 2 sec, 74°C for 30 sec; 30 cycles) and glyceraldehydes-3-phosphate dehydrogenase (GAPDH; 98°C for 10 sec, 57°C for 2 sec, 74°C for 30 sec; 30 cycles), and by using KOD plus (TOYOBO) for TGFα (94°C for 15 sec, 68°C for 1 min; 32 cycles), AR (94°C for 15 sec, 68°C for 1 min; 35 cycles), EPR (94°C for 15 sec, 58°C for 30 sec, 68°C for 30 sec; 35 cycles) and BTC (94°C for 15 sec, 60°C for 30 sec, 68°C for 1 min; 33 cycles). The gene-specific primers are as follows: HB-EGF (5′-ATGAAGCTGCTGCCGTCGGT-3′ and 5′-TCAGTGGGAGCTAGCCACGC-3′), TGFα (5′-ATGGTCCCCGCGACCGGACAGCTCGCTCTG-3′ and 5′-ATCTTCAGACCACTGTCTCAGAGTGGCAGC-3′), AR (5′-ATGAGAACTCCGCTGCTACCGCTGGCGCGC-3′ and 5′-CAGCTAGGCAATGGCGTGCACAGTCCCATT-3′), EPR (5′-CAGGCAGTTATCAGCACAAC-3′, and 5′-CCTTGTCCGTAACTTGATGG-3′), BTC (5′-ATGGACCCAACAGCCCCGGGTAGCAGTGTC-3′ and 5′-TAACCGTTAAGCAATATTGGTCTCTTGAAT-3′), EGF (5′-ATGCCCTGGGGCCGAAGGCCAACCTGGCTG-3′ and 5′-TGTAAGCGTGGCTTCCTTCGCCACTGTCCT-3′), and GAPDH (5′-ACCACAGTCCATGCCATCAC-3′, and 5′-TCCACCACCCTGTTGCTGTA-3′). The optimal cycle number for each gene was determined empirically under unsaturating conditions.

LacZ Staining

Dissected newborn lungs were fixed by perfusion of 0.5% glutaraldehyde-2 mM $MgCl_2$ in PBS (pH 7.4) for 1 hr at 4°C before equilibrating in a sucrose solution (30% sucrose-2 mM $MgCl_2$ in PBS, pH 7.4) overnight at 4°C. Sucrose-infused tissues were embedded in OCT compound and then frozen at −80°C. Eight μm sections were fixed again with 4% paraformaldehyde-2 mM $MgCl_2$ in PBS (pH 7.4) for 10 min at 4°C and then stained with X-gal reaction buffer (containing 35 mM potassium ferrocyanide, 35 mM potassium ferricyanide, 2 mM $MgCl_2$, 0.02% Nonidet P-40, 0.01% Na deoxycholate and 1 mg/ml 5-bromo-4-chloro-3-indolyl-β-D-galactoside in PBS, pH7.4) overnight at 37°C. For *LacZ*

staining of adult lungs, procedures of 0.5% glutaraldehyde perfusion and equilibrating in a sucrose solution were omitted. *LacZ*-stained tissues were counterstained with nuclear fast red.

Hematoxylin and Eosin Staining

Newborns were killed by lethal injection of pentobarbital. Thoraces of embryos and newborns were isolated by decapitation and transection at the level of the liver. Skin and soft tissues were removed and then the intact thoraces were immersed in 4% paraformaldehyde in PBS (pH 7.4) at 4°C for 30 hours. After fixation, heart and lung en bloc was carefully isolated from thoracic cavity without punching the lung or diaphragm to minimize any collapse of the lung. The fixed lungs were dehydrated in graded concentration series of ethanol, and embedded in paraffin. Coronal sections were cut at 4 μm thickness and stained with hematoxylin and eosin.

Lung Morphometry

TSSA were measured as previously described (Shi et al., 1999; Zhao et al., 2001; Yu et al., 2004) by using Adobe Photoshop software. Multiple measurements were performed on randomly selected 0.08-mm^2 image fields acquired from two separate sections greater than 50 μm apart from more than 12 fetal or newborn distal lungs of each genotype (Atkinson et al., 2005). Five fields were selected from one section, including two fields from the cranial lobe of the right lung, two fields from the left lung, and one field from the caudal lobe of the right lung. Fields containing large airways and vessels were avoided. The proportion of lung comprising terminal saccular spaces was calculated as percentage of the total examined area of the lung section.

Measurement of Wet-to-Dry Lung Weight Ratio

After body weights were recorded, newborn lungs were removed intact from the thoracic cavity, blotted free of excess fluid, and weighed. Wet lungs were baked for 24 hr at 65°C. Dried lungs were then weighed (Kramer et al., 2007).

Immunohistochemistry and Quantification

Four-μm lung sections were deparaffinized in xylene, followed by rehydration in series of concentrations of ethanol. The endogenous hydrogen peroxidase was quenched with 6% H_2O_2 for 5 min. Sections were incubated with Ki67 rabbit polyclonal antibody (NCL-Ki67p, Novocastra) diluted 1:500 in blocking solution Block Ace (Dainihon Seiyaku) overnight at 4°C, and then incubated with biotinylated goat anti-rabbit secondary antibody (Vector Laboratories) diluted 1:200 for 30 min at room temperature. Staining was developed using a R.T.U. Vectastain kit (Vector Laboratories) and a diaminobenzidine (DAB) substrate (Merck). Sections were counterstained lightly with hematoxylin. Apoptosis was examined by TUNEL according to the manufacturer's protocol (Promega). After immunostaining with Ki67 or TUNEL staining, randomly selected 0.019 or 0.037 mm^2 image fields acquired from two separate sections greater than 50 μm apart from fetal or newborn distal lungs of each genotype (in total, more than 10 fields from 2 sections of each sample), was captured with the Axiocam digital camera and Axiovision software (Zeiss). An average of 3,285 cells per animal (ranging from 1,543 to 6,022 cells per animal) were counted for this analysis. DAB-stained cells were counted as Ki67- or TUNEL-positive on photographs. The proportion of DAB-positive–stained cells per total cell number was represented as the amount of proliferation or apoptosis.

For pro-surfactant C immunohistochemistry, 4-μm lung sections were deparaffinized in xylene, followed by rehydration in series of concentrations of ethanol. The endogenous hydrogen peroxidase was quenched with 3% H_2O_2 in methanol for 15 min. Sections were incubated with rabbit anti-prosurfactant protein-C (proSP-C) antibody (Chemicon) diluted 1:2,000 in blocking solution (4% goat serum and 0.2% TriotnX-100 in PBS) overnight at 4°C, and then incubated with biotinylated goat anti-rabbit secondary antibody (Vector laboratories) diluted 1:200 for 30 min at room temperature. Staining was developed using the aforementioned R.T.U. Vectastain kit and DAB substrate. Sections were counterstained lightly with Hematoxylin.

Data Analysis

Data are presented as means ± SE. Statistical significance was assessed with Student's *t*-test for paired data, or when necessary, the unpaired *t*-test for unequal variances. A value of $P < 0.05$ was considered statistically significant.

ACKNOWLEDGMENTS

We thank M. Hamaoka and T. Kawaguchi for their technical assistance and advice. R.I. and E.M. were funded by grants-in-aid from the Ministry of Education, Culture, Sports, Science, and Technology and E.M. received a grant-in-aid from Takeda Science Foundation.

REFERENCES

Atkinson JJ, Holmbeck K, Yamada S, Birkedal-Hansen H, Parks WC, Senior RM. 2005. Membrane-type 1 matrix metalloproteinase is required for normal alveolar development. Dev Dyn 232:1079–1090.

Burri PH. 1999. Lung development and pulmonary angionenesis. In: Gaultier C, Bourbon J, Post M, editors. Lung disease. New York: Oxford University Press. p 122–151.

Elenius K, Paul S, Allison G, Sun J, Klagsbrun M. 1997. Activation of HER4 by heparin-binding EGF-like growth factor stimulates chemotaxis but not proliferation. EMBO J 16:1268–1278.

Fowler KJ, Walker F, Alexander W, Hibbs ML, Nice EC, Bohmer RM, Mann GB, Thumwood C, Maglitto R, Danks JA, et al. 1995. A mutation in the epidermal growth factor receptor in waved-2 mice has a profound effect on receptor biochemistry that results in impaired lactation. Proc Natl Acad Sci U S A 92:1465–1469.

Gassmann M, Casagranda F, Orioli D, Simon H, Lai C, Klein R, Lemke G. 1995. Aberrant neural and cardiac development in mice lacking the ErbB4 neuregulin receptor. Nature 378:390–394.

Goishi K, Higashiyama S, Klagsbrun M, Nakano N, Umata T, Ishikawa M, Mekada E, Taniguchi N. 1995. Phorbol ester induces the rapid processing of cell surface heparin-binding EGF-like growth factor: conversion from juxta-

crine to paracrine growth factor activity. Mol Biol Cell 6:967–980.
Harris RC, Chung E, Coffey RJ. 2003. EGF receptor ligands. Exp Cell Res 284:2–13.
Hashimoto K, Higashiyama S, Asada H, Hashimura E, Kobayashi T, Sudo K, Nakagawa T, Damm D, Yoshikawa K, Taniguchi N. 1994. Heparin-binding epidermal growth factor-like growth factor is an autocrine growth factor for human keratinocytes. J Biol Chem 269:20060–20066.
Higashiyama S, Abraham JA, Miller J, Fiddes JC, Klagsbrun M. 1991. A heparin-binding growth factor secreted by macrophage-like cells that is related to EGF. Science 251:936–939.
Holbro T, Hynes NE. 2004. ErbB receptors: directing key signaling networks throughout life. Annu Rev Pharmacol Toxicol 44:195–217.
Iwamoto R, Mekada E. 2000. Heparin-binding EGF-like growth factor: a juxtacrine growth factor. Cytokine Growth Factor Rev 11:335–344.
Iwamoto R, Mekada E. 2006. ErbB and HB-EGF signaling in heart development and function. Cell Struct Funct 31:1–14.
Iwamoto R, Yamazaki S, Asakura M, Takashima S, Hasuwa H, Miyado K, Adachi S, Kitakaze M, Hashimoto K, Raab G, Nanba D, Higashiyama S, Hori M, Klagsbrun M, Mekada E. 2003. Heparin-binding EGF-like growth factor and ErbB signaling is essential for heart function. Proc Natl Acad Sci U S A 100: 3221–3226.
Jackson LF, Qiu TH, Sunnarborg SW, Chang A, Zhang C, Patterson C, Lee DC. 2003. Defective valvulogenesis in HB-EGF and TACE-null mice is associated with aberrant BMP signaling. EMBO J 22:2704–2716.
Kimura R, Iwamoto R, Mekada E. 2005. Soluble form of heparin-binding EGF-like growth factor contributes to retinoic acid-induced epidermal hyperplasia. Cell Struct Funct 30:35–42.
Kramer EL, Deutsch GH, Sartor MA, Hardie WD, Ikegami M, Korfhagen TR, Le Cras TD. 2007. Perinatal increases in TGF-{alpha} disrupt the saccular phase of lung morphogenesis and cause remodeling: microarray analysis. Am J Physiol Lung Cell Mol Physiol 293:L314–L27.
Kubiak J, Mitra MM, Steve AR, Hunt JD, Davies P, Pitt BR. 1992. Transforming growth factor-alpha gene expression in late-gestation fetal rat lung. Pediatr Res 31:286–290.
Luetteke NC, Phillips HK, Qiu TH, Copeland NG, Earp HS, Jenkins NA, Lee DC. 1994. The mouse waved-2 phenotype results from a point mutation in the EGF receptor tyrosine kinase. Genes Dev 8: 399–413.
Massague J, Pandiella A. 1993. Membrane-anchored growth factors. Annu Rev Biochem 62:515–541.
Miettinen PJ, Berger JE, Meneses J, Phung Y, Pedersen RA, Werb Z, Derynck R. 1995. Epithelial immaturity and multiorgan failure in mice lacking epidermal growth factor receptor. Nature 376:337–341.
Miettinen PJ, Warburton D, Bu D, Zhao JS, Berger JE, Minoo P, Koivisto T, Allen L, Dobbs L, Werb Z, Derynck R. 1997. Impaired lung branching morphogenesis in the absence of functional EGF receptor. Dev Biol 186:224–236.
Mine N, Iwamoto R, Mekada E. 2005. HB-EGF promotes epithelial cell migration in eyelid development. Development 132: 4317–4326.
Miyamoto S, Yagi H, Yotsumoto F, Kawarabayashi T, Mekada E. 2006. Heparin-binding epidermal growth factor-like growth factor as a novel targeting molecule for cancer therapy. Cancer Sci 97:341–347.
Piepkorn M, Pittelkow MR, Cook PW. 1998. Autocrine regulation of keratinocytes: the emerging role of heparin-binding, epidermal growth factor-related growth factors. J Invest Dermatol 111: 715–721.
Raab G, Klagsbrun M. 1997. Heparin-binding EGF-like growth factor. Biochim Biophys Acta 1333:F179–F199.
Roth-Kleiner M, Hirsch E, Schittny JC. 2004. Fetal lungs of tenascin-C-deficient mice grow well, but branch poorly in organ culture. Am J Respir Cell Mol Biol 30:360–366.
Ruocco S, Lallemand A, Tournier JM, Gaillard D. 1996. Expression and localization of epidermal growth factor, transforming growth factor-alpha, and localization of their common receptor in fetal human lung development. Pediatr Res 39:448–455.
Shi W, Heisterkamp N, Groffen J, Zhao J, Warburton D, Kaartinen V. 1999. TGF-beta3-null mutation does not abrogate fetal lung maturation in vivo by glucocorticoids. Am J Physiol 277:L1205–L1213.
Shirakata Y, Kimura R, Nanba D, Iwamoto R, Tokumaru S, Morimoto C, Yokota K, Nakamura M, Sayama K, Mekada E, Higashiyama S, Hashimoto K. 2005. Heparin-binding EGF-like growth factor accelerates keratinocyte migration and skin wound healing. J Cell Sci 118:2363–2370.
Sibilia M, Wagner EF. 1995. Strain-dependent epithelial defects in mice lacking the EGF receptor. Science 269:234–238.
Strandjord TP, Clark JG, Hodson WA, Schmidt RA, Madtes DK. 1993. Expression of transforming growth factor-alpha in mid-gestation human fetal lung. Am J Respir Cell Mol Biol 8:266–272.
Strandjord TP, Clark JG, Madtes DK. 1994. Expression of TGF-alpha, EGF, and EGF receptor in fetal rat lung. Am J Physiol 267:L384–L389.
Strandjord TP, Clark JG, Guralnick DE, Madtes DK. 1995. Immunolocalization of transforming growth factor-alpha, epidermal growth factor (EGF), and EGF-receptor in normal and injured developing human lung. Pediatr Res 38:851–856.
Ten Have-Opbroek AA. 1991. Lung development in the mouse embryo. Exp Lung Res 17:111–130.
Tidcombe H, Jackson-Fisher A, Mathers K, Stern DF, Gassmann M, Golding JP. 2003. Neural and mammary gland defects in ErbB4 knockout mice genetically rescued from embryonic lethality. Proc Natl Acad Sci U S A 100:8281–8286.
Yamazaki S, Iwamoto R, Saeki K, Asakura M, Takashima S, Yamazaki A, Kimura R, Mizushima H, Moribe H, Higashiyama S, Endoh M, Kaneda Y, Takagi S, Itami S, Takeda N, Yamada G, Mekada E. 2003. Mice with defects in HB-EGF ectodomain shedding show severe developmental abnormalities. J Cell Biol 163: 469–475.
Yu H, Wessels A, Chen J, Phelps AL, Oatis J, Tint GS, Patel SB. 2004. Late gestational lung hypoplasia in a mouse model of the Smith-Lemli-Opitz syndrome. BMC Dev Biol 4:1.
Zhao J, Chen H, Peschon JJ, Shi W, Zhang Y, Frank SJ, Warburton D. 2001. Pulmonary hypoplasia in mice lacking tumor necrosis factor-alpha converting enzyme indicates an indispensable role for cell surface protein shedding during embryonic lung branching morphogenesis. Dev Biol 232:204–218.

Available online at www.sciencedirect.com
ScienceDirect
Biochemical and Biophysical Research Communications 365 (2008) 555–561
BBRC
www.elsevier.com/locate/ybbrc

Validation of HB-EGF and amphiregulin as targets for human cancer therapy

Fusanori Yotsumoto [a], Hiroshi Yagi [c], Satoshi O. Suzuki [d], Eiji Oki [e], Hiroshi Tsujioka [a], Touru Hachisuga [f], Kenzo Sonoda [c], Tatsuhiko Kawarabayashi [a], Eisuke Mekada [g], Shingo Miyamoto [b,*]

[a] *Department of Obstetrics and Gynecology, School of Medicine, Fukuoka University, Fukuoka, Japan*
[b] *Department of Biochemistry, School of Medicine, Fukuoka University, 45-1, 7-chome, Nanakuma, Jyounan-ku, Fukuoka 814-0180, Japan*
[c] *Department of Obstetrics and Gynecology, Graduate School of Medical Sciences, Kyushu University, Fukuoka, Japan*
[d] *Department of Neuropathology, Graduate School of Medical Sciences, Kyushu University, Fukuoka, Japan*
[e] *Department of Surgery and Sciences, Graduate School of Medical Sciences, Kyushu University, Fukuoka, Japan*
[f] *Department of Obstetrics and Gynecology, School of Medicine, University of Occupational and Environmental Health, Kitakyushu, Japan*
[g] *Department of Cell Biology, Research Institute for Microbial Diseases, Osaka University, Osaka, Japan*

Received 27 October 2007
Available online 20 November 2007

Abstract

Aberrant expression levels of epidermal growth factor receptor (EGFR) and its cognate ligands have been recognized as one of the causes of cancer progression. To investigate the validity of EGFR ligands as targets for cancer therapy, we examined the expression of EGFR ligands and in vitro anti-tumor effects of small interference RNA (siRNA) for EGFR ligands in various cancer cells. HB-EGF expression was dominantly elevated in ovarian, gastric, and breast cancer, melanoma and glioblastoma cells, whereas amphiregulin was primarily expressed in pancreatic, colon, and prostate cancer, renal cell carcinoma and cholangiocarcinoma cells. Transfection of siRNAs for HB-EGF or amphiregulin into these cells significantly increased the numbers of apoptotic cells with attenuation of EGFR and ERK activation. In lung cancer cells, any EGFR ligand was not recognized as a validated target for cancer therapy. These results suggest that HB-EGF and amphiregulin are promising targets for cancer therapy.

Keywords: HB-EGF; Amphiregulin; EGFR; Human cancer; Targeting therapy

Epidermal growth factor receptor (EGFR), which belongs to the ErbB family, plays pivotal roles in the diverse processes of proliferation and differentiation [1]. Aberrant activation of EGFR signaling, such as that due to overexpression of EGFR or abnormal stimulation by autocrine growth factor loops, can contribute to constitutive EGFR signaling, resulting in dysregulation of cell growth and cancer [2]. Overexpression of EGFR has been considered to represent a poor prognostic factor in many human cancers, including ovarian, endometrial, breast, gastric, bladder, lung, pancreatic, and colon cancers, renal cell carcinoma, cholangiocarcinoma, and cervical adenocarcinoma, as well as glioblastoma and malignant melanoma [3]. Accordingly, EGFR represents a validated therapeutic target for the treatment of these human cancers and this has resulted in the development of multiple therapeutics, including the antibody cetuximab and other anti-EGFR antibodies as well as ATP-competitive tyrosine kinase inhibitors, such as erlotinib and gefitinib [4]. These EGFR-targeted therapies have improved the efficacies of conventional chemotherapy in both preclinical and clinical studies [5]. Although such therapies may lead to a partial response or disease stabilization in some patients, many

* Corresponding author. Fax: +81 92 801 3600.
E-mail address: smiya@cis.fukuoka-u.ac.jp (S. Miyamoto).

0006-291X/$ - see front matter © 2007 Elsevier Inc. All rights reserved.
doi:10.1016/j.bbrc.2007.11.015

patients do not benefit from EGFR-targeted therapies and those who do benefit eventually develop resistance to the administered therapy.

EGFR is activated by a number of ligands, termed epidermal growth factor (EGF)-related peptide growth factors [6]. The ligands identified to date include EGF, amphiregulin, epigen, and transforming growth factor-α (TGF-α), which bind specifically to EGFR, and betacellulin, heparin-binding EGF-like growth factor (HB-EGF), and epiregulin, which exhibit dual specificity for EGFR and ErbB4 [7]. In contrast to their receptors, the ligands that comprise the EGF family of growth factors have not yet been focused on as targets for cancer therapy. This is possibly due to the redundancy of EGFR ligands for each receptor, which has led to a general consensus that inhibiting receptor function is more effective than inhibiting multiple ligands for cancer therapy. However, recent studies have suggested that high EGFR ligand concentrations can circumvent the effectiveness of EGFR-targeted agents or the less selective ErbB kinase inhibitors. In addition to these lines of evidence, HB-EGF has been proposed as a promising target for ovarian cancer [8]. On the basis of these results, it is possible that EGFR ligands may be considered as valuable target molecules for cancer therapy.

To investigate the validity of EGFR ligands as targets for human cancer, we examined the expressions of all the known EGFR ligands and the *in vitro* anti-tumor effects of suppressing these EGFR ligands in a variety of human cancer cells.

Materials and methods

Reagents. Diphtheria toxin was prepared as described previously [9]. All the siRNAs for EGFR ligands and EGFR were purchased from TaKaRa Bio Inc. (Shiga, Japan). Polyclonal rabbit anti-EGFR (sc03) and anti-ERK1/2 antibodies were purchased from Santa Cruz Biotechnology (Santa Cruz, CA). Mouse monoclonal antibodies against phospho-tyrosine clone 4G10 and phospho-MAPK were acquired from Upstate Biotechnology Inc. (Lake Placid, NY).

Cells and cell culture. The following cell lines were obtained commercially: HuH7 cells from the Cell Resource Center for Biomedical Research (Institute of Development, Aging and Cancer, Tohoku University, Sendai, Japan); RMG1, TYK-nu, and MKN28 cells from the Japanese Collection of Research Bioresources (Osaka, Japan); SKOV3, PA-1, T24, NUGC3, G361, HT29, HCT116, COLO201, LoVo, WiDr, LS180, ASPC1, PC-3, Du145, U251MG, Caki-1, MDA-MB-231, and NCI-H460 cells from the American Type Culture Collection (Manassas, VA). The OVMG1 cell line was kindly gifted by Dr. H. Kobayashi (Kyushu University, Fukuoka, Japan). All cells were maintained in RPMI1640 medium supplemented with 10% fetal bovine serum (ICN Biomedicals, Irvine, CA), 100 U/ml of penicillin G and 100 μg/ml of streptomycin (Invitrogen Corp., Carlsbad, CA) in a humidified atmosphere of 5% CO_2 at 37 °C.

Performance of real-time quantitative PCR for EGFR ligands and EGFR. RNA extraction and cDNA synthesis were performed using TRIzol and SuperScript II reverse transcriptase (Invitrogen Corp.), respectively, according to the manufacturer's protocols. The primer and probe sequences for EGF and epigen were as follows: EGF forward primer, 5′-CTT TGC CTT GCT CTG TCA CAG T-3′; EGF reverse primer, 5′-AAT ACC TGA CAC CCT TAT GAC AAA TTT-3′; EGF probe, 5′-AAG TCA GCC AGA GCA GGG CTG TTA AAC TCT-3′; epigen forward primer, 5′-TCT ATC TTT TAT TCA ACG CAA TGA CA-3′; epigen reverse primer, 5′-GGG CTG TGA TTG GAG GTG TT-3′; epigen probe, 5′-ACT GAC CGA AGA GGC AGC CGT GAC T-3′. Glyceraldehyde-3-phosphate dehydrogenase (GAPDH) and EGFR were detected with Assays-on-Demand primer and probe sets Hs99999905_m1 and Hs00193306_m1, respectively (Applied Biosystems, Foster City, CA). The procedures used for TaqMan quantitative real-time PCR analyses as well as the sequences of the oligonucleotide primer pairs, TaqMan probes for HB-EGF, amphiregulin, TGF-α, epiregulin, and betacellulin and the calculation for mRNA EI were described previously [10]. All experiments were carried out independently three times.

Soluble HB-EGF, amphiregulin, EGF, and TGF-α in cell culture medium. Cells were seeded on 10-cm dishes (50–60% confluence) and incubated for 48 h. Each culture medium (CM) and the soluble forms of HB-EGF and amphiregulin bound to extracellular matrices on the cell surface (CSS) were completely collected according to the following procedures [11]. The levels of EGF, TGF-α, and amphiregulin were determined using a commercially available sandwich ELISA (DuoSet Kit; R&D Systems Inc., Minneapolis, MN) in accordance with the manufacturer's instructions. The concentration of HB-EGF in each sample was measured using a previously described binding assay [12]. Since the amounts of EGF, TGF-α, and amphiregulin in the CSS could not be directly detected due to the high salt concentration, the amounts of these EGFR ligands were measured after 10-fold dilution of the samples in a diluent (137 mM NaCl, 2.7 mM KCl, 10 mM phosphate buffer, and 10 mg/ml bovine serum albumin). In measuring the amounts of EGF, TGF-α, and amphiregulin in the CSS, the lower limits for detection were 39, 78, and 156 pg/ml, respectively. When the level was less than the detection limit, value of EGF, TGF-α, or amphiregulin was recorded as 39, 78, or 156 pg/ml, respectively. Samples were assayed in triplicate. Each mean value was considered as representative for the CM or CSS.

Transfections of siRNAs for EGFR ligands and EGFR. Cells (4×10^5) were seeded on polylysine-coated 6-cm dishes (50–60% confluence). The siRNAs for the EGFR ligands and EGFR were individually transfected into cells using TransIT-TKO (Mirus, Madison, WI) according to the manufacturer's instructions. The final concentration of each siRNA for transfection was 20 μM. After incubation for 72 h, the cells were subjected to apoptosis assays, immunoprecipitation, and immunoblot analyses.

Cell apoptosis assay. Cells were harvested, pooled, and fixed with 4% paraformaldehyde at 4 °C for 30 min and resuspended in 70% ethanol at −20 °C for 30 min. After washing in phosphate-buffered saline (PBS), the cells were incubated with TdT reaction reagent (MEBSTAIN Apoptosis Kit Direct; MBL Co. Ltd., Nagoya, Japan) for 1 h at 37 °C, according to the manufacturer's instructions. TUNEL-positive cells were quantified as apoptotic cells by flow cytometric analysis using a FACScalibur (Becton–Dickinson, Franklin Lakes, NJ).

Immunoprecipitation and immunoblot analyses. Cells were rinsed in PBS containing 1 mM sodium orthovanadate and lysed with 0.3 ml of RIPA buffer (1% Triton X-100, 1% sodium deoxycholate, 0.1% SDS, 150 mM NaCl, 50 mM Tris, pH 8.0, 0.2 U/ml aprotinin, 2 mM phenylmethylsulfonyl fluoride, and 1 mM sodium orthovanadate). Extracts and immunoprecipitates were subjected to SDS–polyacrylamide gel electrophoresis and immunoblotting analysis as described previously [8].

Statistical analysis. The statistical significance of differences between values was assessed using the Mann–Whitney U test. Values of $P < 0.05$ were considered statistically significant.

Results

mRNA expression of EGFR ligands, EGFR, and ErbB2 as well as secretion of EGFR ligand proteins in cancer cell lines

HB-EGF or amphiregulin was identified as the primarily predominant EGFR ligand in most of cancer cells, whereas the expression levels of the other EGFR ligands appeared to vary (Fig. 1A and B, and Supplemental Fig. 1A–L). In ovarian, gastric, bladder, and breast cancers, malignant

melanoma and glioblastoma cells with high expression of HB-EGF mRNA, and abundant secretion of soluble HB-EGF were found (Fig. 2A and Supplemental Fig. 2A). In colon, pancreatic, and prostate cancer, renal cell carcinoma, hepatocellular carcinomas, and cholangiocarcinoma cells, amphiregulin was also prominently secreted by the cells (Fig. 2B and Supplemental Fig. 2B). In lung cancer cells, enhanced production of a mutual EGFR ligand was not found (Supplemental Fig. 1M and Fig. 2C). The fraction bound to the cell surface contained a significant amount of HB-EGF, whereas the level of amphiregulin was quite low in the CSS. None of the cancer cell lines examined showed significant production of TGF-α or EGF. In flow cytometric analyses, U373MG, U251MG, KNS81, and U118MG cells had positive expression of HB-EGF in more than 15% of cells, whereas positive expression of TGF-α was found in <3% of these cells. Similarly, Caki-1, ACHN, and SW839 cells showed positive expression of amphiregulin in more than 15% of cells, although positive expression of epiregulin was in the range of 5% of these cells. Taken together, these results suggest that HB-EGF and amphiregulin function as autocrine or paracrine EGF-related peptides in human cancer.

Significance of EGFR ligands in signaling and in vitro antitumor effects

To elucidate whether HB-EGF and amphiregulin play key roles in EGFR signaling, suppression of EGFR and ERK activation were examined after transfection of siRNAs for HB-EGF, amphiregulin, or EGFR. In RMG1 or LoVo cells, the introduction of a siRNA for HB-EGF or amphiregulin attenuated the activation of EGFR and ERK, compared to siRNAs for EGFR and other EGFR ligands (Fig. 3A and B). In gastric, bladder, and breast cancer, and glioblastoma cells with predominant expression of

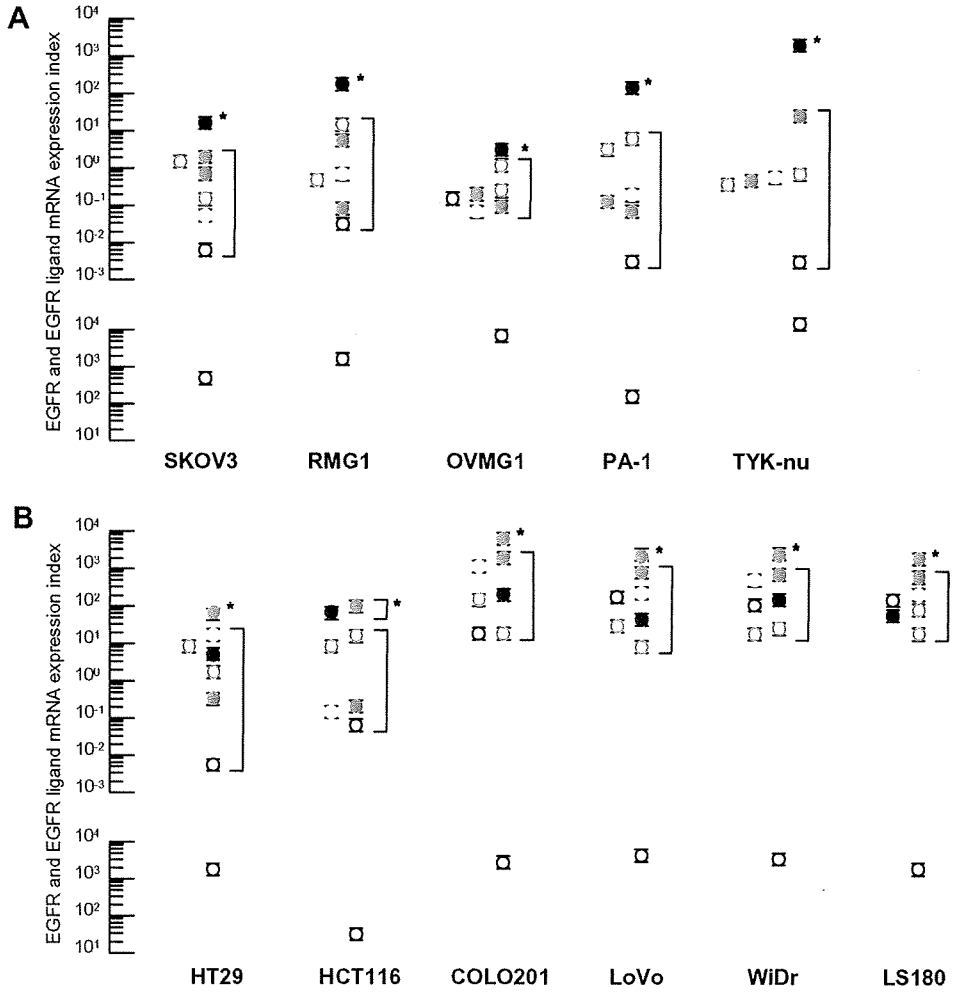

Fig. 1. Differences in the expressions of EGFR ligands, EGFR in ovarian (A) and colon cancer (B) cell lines. The mRNA expression indexes in the cancer cells are coded as follows: HB-EGF, closed red circles; amphiregulin, closed blue circles; TGF-α, closed yellow circles; EGF, open red circles; epiregulin, closed green circles; betacellulin, open blue circles; epigen, open green circles; EGFR, open black circles. Each value represents the mean and standard deviation of the mRNA expression index for an EGFR ligand or EGFR. $^{*}P < 0.05$, versus the values of the other EGFR ligands. (For interpretation of the references to colour in this figure legend, the reader is referred to the web version of this article.)

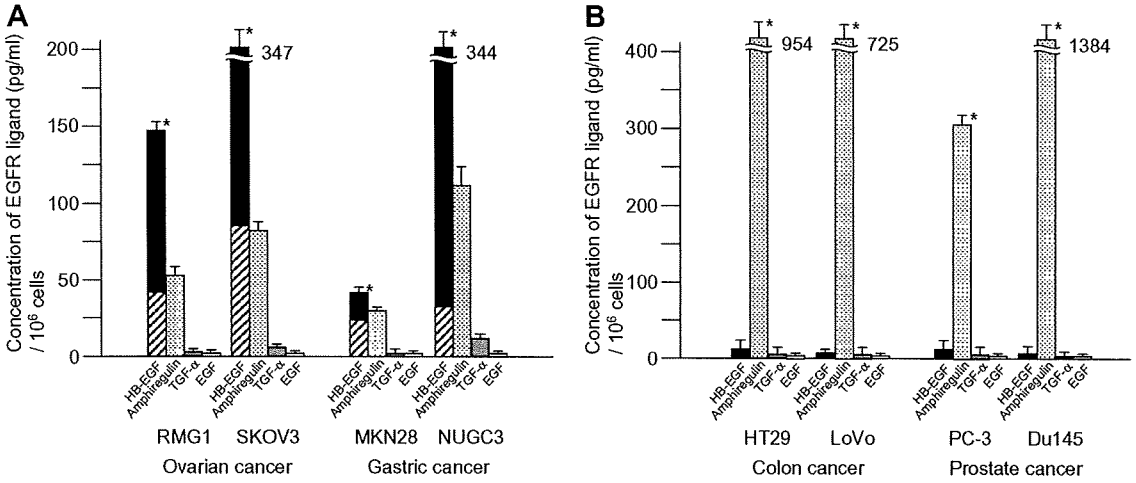

Fig. 2. Protein levels of EGFR ligands in CM and CSS samples from cancer cell lines cultured for 48 h. Each concentration of HB-EGF, amphiregulin, TGF-α, and EGF is presented as the concentration per 1×10^6 cells. Closed bars, HB-EGF in CM; hatched bars, HB-EGF in CSS; dotted bars, amphiregulin; gray bars, TGF-α; open bars, EGF Predominant expression of HB-EGF is detected in ovarian and gastric cancer cells (A) as well as colon and prostate cancer cells (B) ($^*P < 0.05$ for HB-EGF or amphiregulin versus other EGFR ligands). Bars indicate the means of three independent experiments and vertical lines indicate the standard deviations.

HB-EGF, suppression of HB-EGF expression, like EGFR, decreased the expression of tyrosine-phosphorylated EGFR or ERK, whereas transfection of siRNAs for other EGFR ligands did not inhibit the activation of EGFR or ERK (Supplemental Fig. 3A). In pancreatic cancer, renal cell carcinoma, and hepatocellular carcinoma cells with abundant expression of amphiregulin, suppression of EGFR and ERK activation was mediated by inhibition of amphiregulin, compared to the suppression of other EGFR ligands or even EGFR itself (Supplemental Fig. 3B). In RMG1, MNK28, T24, U251MG, and MDA-MB-231 cells, the amounts of soluble HB-EGF in the CM or CSS were decreased by approximately 20–40% after transfection of a siRNA for HB-EGF. The levels of amphiregulin in the CM and CSS were also decreased by 20–40% in LoVo, ASPC1, Caki-1, and HuH7 cells after transfection of a siRNA for amphiregulin. To confirm HB-EGF and amphiregulin as valid targets for cancer therapy, cell apoptosis was examined following suppression of HB-EGF or amphiregulin. Suppression of HB-EGF or amphiregulin induced significant apoptosis of RMG1 MKN28, T24, U251MG, G361, and MDA-MB-231 cells or LoVo, ASPC1, and Caki-1 cells (Table 1 and Supplemental Fig. 4). Although introduction of a siRNA for amphiregulin into HuH7 cells suppressed the activation of EGFR and ERK, it did not augment the number of apoptotic cells, compared with other siRNAs. In NCI-H460 cells, no significant alterations in activation of EGFR as well as ERK and in number of apoptotic cells were found through the transfection of siRNAs for EGFR and its cognate ligands (Table 1 and Supplemental Fig. 3C).

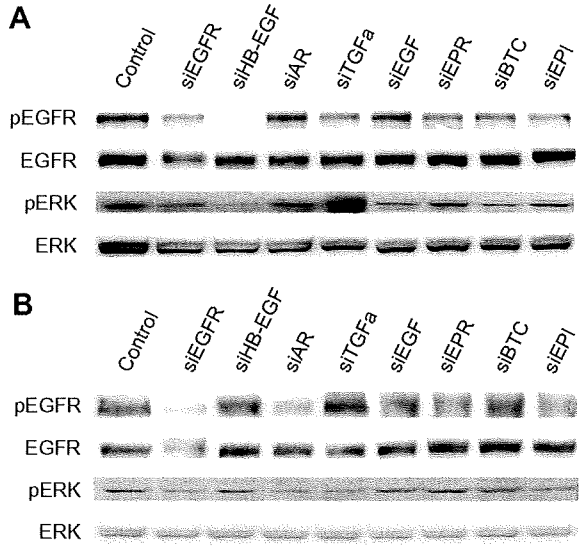

Fig. 3. Alterations in the tyrosine phosphorylation of EGFR and ERK. siRNAs for EGFR ligands and EGFR were individually transfected into RMG1 (A) and LoVo (B) cells. Top two panels, lysates were immunoprecipitated with antibodies specific for EGFR, and the immunoprecipitates were probed with antibodies against phospho-tyrosine or EGFR. Bottom two panels, lysates were immunoblotted with antibodies against phospho-ERK (pERK) and ERK.

Discussion

In the present study, we have confirmed the validity of HB-EGF and amphiregulin as targets for cancer therapy (Supplemental Table 1). HB-EGF and amphiregulin possess a heparin-binding motif, whereas the other EGFR ligands do not [7]. Accordingly, HB-EGF and amphiregulin have quite an advantage toward accumulating on the cell surface and activating the EGFR pathway through binding to heparin sulfate proteoglycans (HSPGs) com-

Table 1
Flow cytometric analysis of apoptotic cells among cancer cell lines transiently transfected with siRNAs for EGFR or EGFR ligands

Ligands	Cell line	siRNA				
		EGFR	HB-EGF	Amphiregulin	TGF-α	Epiregulin
Ovarian cancer	RMG1	$9.01 \pm 0.98^{*}$	$13.15 \pm 0.92^{**}$	2.79 ± 1.05	2.35 ± 0.28	1.36 ± 0.62
Gastric cancer	MKN28	$5.57 \pm 1.15^{*}$	$16.24 \pm 3.54^{**}$	4.37 ± 1.04	2.12 ± 0.49	N.D.
Bladder cancer	T24	$4.24 \pm 0.60^{*}$	$7.04 \pm 1.37^{**}$	3.28 ± 0.93	2.74 ± 0.40	N.D.
Glioblastoma	U251MG	$4.05 \pm 0.40^{*}$	$4.51 \pm 0.87^{*}$	3.18 ± 0.41	2.65 ± 1.25	N.D.
Malignant melanoma	G361	$3.44 \pm 0.32^{*}$	$3.78 \pm 0.25^{*}$	1.52 ± 0.89	0.25 ± 0.25	N.D.
Breast cancer	MDA-MB-231	$4.47 \pm 0.34^{*}$	$7.31 \pm 0.93^{**}$	2.56 ± 1.03	1.72 ± 1.11	N.D.
Colon cancer	LoVo	$9.25 \pm 1.46^{***}$	2.79 ± 0.76	$13.25 \pm 3.35^{***}$	3.58 ± 0.92	3.72 ± 1.16
Pancreatic cancer	ASPC1	$3.35 \pm 0.71^{****}$	0.04 ± 0.06	$8.27 \pm 1.06^{***}$	N.D.	1.87 ± 0.81
Prostate cancer	PC-3	$7.75 \pm 3.68^{*****}$	$8.16 \pm 2.74^{*****}$	$7.12 \pm 1.61^{*****}$	N.D.	3.36 ± 1.46
Renal cell carcinoma	Caki-1	$15.25 \pm 3.25^{******}$	4.74 ± 0.72	$8.12 \pm 1.49^{***}$	N.D.	3.34 ± 1.12
Hepatocellular carcinoma	HuH7	4.21 ± 0.87	4.02 ± 0.27	3.81 ± 1.18	N.D.	3.89 ± 0.97
Lung cancer	NCI-H460	1.75 ± 0.68	0.66 ± 0.14	0.82 ± 0.61	1.36 ± 0.46	1.03 ± 0.58

Notes. Values are means (%) ± SD of three independent experiments. N.D.: Not done.

* $P < 0.05$ versus RMG1, MKN28, T24, U251MG, G361, and MDA-MB-231 cells for cells transfected with siRNAs for amphiregulin and TGF-α, respectively.

** $P < 0.05$ versus RMG1, MKN28, T24 and MDA-MB-231 cells for cells transfected with a siRNA for EGFR.

*** $P < 0.05$ versus LoVo, ASPC1, and Caki-1 cells for cells transfected with siRNAs for HB-EGF and epiregulin, respectively.

**** $P < 0.05$ versus ASPC1 cells for cells transfected with a siRNA for EGFR.

***** $P < 0.01$ versus PC-3 cells for cells transfected with a siRNA for epiregulin.

****** $P < 0.05$ versus Caki-1 cells for cells transfected with a siRNA for amphiregulin.

pared to other EGFR ligands without the motif, although a difference between the affinities of HB-EGF and amphiregulin for HSPGs was found in the present study. HB-EGF and amphiregulin, which have broad spectra of biological activities including wound healing, blast implantation, and tumor formation [13–15], are defined as immediate-early response genes and may play key roles in mediating the earliest cellular responses to proliferative stimuli [16]. Thus, there are large differences in the structures and functions of HB-EGF and amphiregulin compared to the other EGFR ligands. In addition, activation of Ras or Raf on the EGFR-Ras-Raf-ERK axis enhances the expressions of HB-EGF and amphiregulin [17–19], although Ras and Raf are also regarded as promising targets for cancer therapy [20]. Activation of intracellular signaling in EGFR pathways requires EGFR for tumorigenic properties [21]. According to these lines of evidence, it is plausible that EGFR, as well as HB-EGF or amphiregulin, is indispensable for malignant transformation of human epithelial cells.

HB-EGF-null mice show quite severe phenotypes in their cardiovascular systems [22]. Although transgenic expression of HB-EGF accelerates the proliferation of hepatocytes after partial hepatectomy [23], there have been no reports that HB-EGF is involved in the development of melanocytes or epithelia in the ovary, endocervix, endometrium, or stomach. Amphiregulin-knockout mice show impaired proliferative responses after partial liver resection and female mice exhibit impaired mammary gland development and/or function [24,25]. Neonatal mice lacking amphiregulin, EGF, and TGF-α display spontaneous duodenal lesions, while the alveoli in the triple null mammary glands are poorly organized and differentiated [26]. Accordingly, it is plausible that amphiregulin is involved in the development of cancers originating from the colon and liver. Amphiregulin transgenic mice display small intralobular ducts and centroacinar cell proliferation, suggesting that amphiregulin may be involved in the proliferation of pancreatic duct cells [27]. EGF-, epiregulin-, betacellulin-, or TGF-α-knockout mice are healthy and fertile and display no significantly adverse phenotypic effects [24,28–31]. Mice overexpressing betacellulin exhibit severe alterations of the lung, accompanied by high early postnatal mortality, while EGF transgenic mice display no definite phenotypes [32,33]. There have been no reports regarding the phenotypes of knockout or transgenic mice for epigen or epiregulin transgenic mice. On the basis of these pieces of evidence, it remains unsolved why HB-EGF or amphiregulin is recognized as the predominantly expressed EGFR ligand in cancer cells originating from individual organs.

Autocrine/paracrine production of EGFR ligands and overexpression of EGFR are two of the most frequent mechanisms implicated in cancer development and progression. In addition, aberrant enhancement of EGFR ligand expression is speculated to be one of several different molecular mechanisms, including receptor mutations, constitutive activation of downstream pathways, and activation of alternative pathways, for the acquired resistance against EGFR antagonists [34]. Thus, a particular EGFR ligand that is predominantly expressed in human cancer can be recognized as a more valid target than EGFR itself. The results of the present study have demonstrated that HB-EGF and amphiregulin represent key EGFR ligands in human cancers. Based on these pieces of evidence, the development of therapeutic agents against HB-EGF or amphiregulin may allow us to improve the clinical outcomes of patients with cancer.

Acknowledgments

This work was supported in part by a Grant-in-Aid for Scientific Research on Priority Areas (No. 17014057) and Research Promotion for Innovative Therapies against Cancers from the Ministry of Education, Culture, Sports, Science and Technology to E.M.

Appendix A. Supplementary data

Supplementary data associated with this article can be found, in the online version, at doi:10.1016/j.bbrc.2007.11.015.

References

[1] A. Citri, Y. Yarden, EGF-ERBB signaling: towards the systems level, Nat. Rev. Mol. Cell Biol. 7 (2006) 505–516.
[2] N.E. Hynes, H.A. Lane, ERBB receptors and cancer: the complexity of targeted inhibitors, Nat. Rev. Cancer 5 (2005) 341–354.
[3] D.S. Salomon, R. Brandt, F. Ciardiello, N. Normanno, Epidermal growth factor-related peptides and their receptors in human malignancies, Crit. Rev. Oncol. Hematol. 19 (1995) 183–232.
[4] J. Baselga, C.L. Artaga, Critical update and emerging trends in epidermal growth factor receptor targeting in cancer, J. Clin. Oncol. 23 (2005) 2445–2459.
[5] C.M. Roch-Lima, H.P. Soares, L.E. Raez, R. Singal, EGFR targeting of solid tumors, Cancer Control 14 (2007) 295–304.
[6] D.J. Riese II, D.F. Stern, Specificity within the EGF family/ErbB receptor family signaling network, BioEssays 20 (1998) 41–48.
[7] R.C. Harris, E. Chung, R.J. Coffey, EGF receptor ligands, Exp. Cell Res. 284 (2003) 2–13.
[8] S. Miyamoto, M. Hirata, A. Yamazaki, T. Kageyama, H. Hasuwa, H. Mizushima, Y. Tanaka, H. Yagi, K. Sonoda, M. Kai, H. Kanoh, H. Nakano, E. Mekada, Heparin-binding EGF-like growth factor is a promising target for ovarian cancer therapy, Cancer Res. 64 (2004) 5720–5727.
[9] T. Uchida, A.M. Pappenheimer Jr., R. Greany, Diphtheria toxin and related proteins, J. Biol. Chem. 248 (1973) 3838–3844.
[10] Y. Tanaka, S. Miyamoto, S.O. Suzuki, E. Oki, H. Yagi, K. Sonoda, A. Yamazaki, H. Mizushima, Y. Maehara, E. Mekada, H. Nakano, Clinical significance of heparin-binding growth factor-like growth factor and a disintegrin and metalloprotease 17 expression in human ovarian cancer, Clin. Cancer Res. 11 (2005) 4783–4792.
[11] S. Higashiyama, R. Iwamoto, K. Goishi, G. Raab, N. Taniguchi, M. Klagsbrun, E. Mekada, The membrane protein CD9/DRAP 27 potentiates the juxtacrine growth factor activity of the membrane-anchored heparin-binding EGF-like growth factor, J. Cell Biol. 128 (1995) 929–938.
[12] H. Yagi, S. Miyamoto, Y. Tanaka, K. Sonoda, H. Kobayashi, T. Kishikawa, R. Iwamoto, E. Mekada, H. Nakano, Clinical significance of heparin-binding epidermal growth factor-like growth factor in peritoneal fluid of ovarian cancer, Br. J. Cancer 92 (2005) 1737–1745.
[13] V.R.J. Schelfhout, E.D. Coene, B. Delaey, A.A.T. Waeytens, L.D. Rycke, M. Deleu, C.R. De Potter, The role of heregulin-α as a motility factor and amphiregulin as a growth factor in wound healing, J. Pathol. 198 (2002) 523–533.
[14] Y. Shirakata, R. Kimura, D. Nanba, R. Iwamoto, S. Tokumaru, C. Morimoto, K. Yokota, M. Nakamura, K. Sayama, E. Mekada, S. Higahiyama, K. Hashimoto, Heparin-binding EGF-like growth factor accelerates keratinocyte migration and skin wound healing, J. Cell Sci. 118 (2005) 2363–2370.
[15] D.S. Lee, Y. Yanagimoto-Ueta, H. Suzuki, Expression of amphiregulin during the pre- and post- implantation period in the mouse reproductive tract, J. Reprod. Dev. 52 (2006) 781–787.
[16] J.A. Barnard, R.D. Beauchamp, W.E. Russell, R.N. Dubois, R.J. Coffey, Epidermal growth factor-related peptides and their relevance to gastrointestinal pathophysiology, Gastroenterology 108 (1995) 564–580.
[17] S.A. McCarthy, M.L. Samuels, C.A. Pritchard, J.A. Abraham, M. McMahon, Rapid induction of heparin-binding epidermal growth factor/diphtheria toxin receptor expression by Raf and Ras oncogenes, Genes Dev. 9 (1995) 1953–1964.
[18] L.M. Gangarosa, N. Sizemore, R. Graves-Deal, S.M. Oldham, C.J. Der, J.C. Robert, A Raf-independent epidermal growth factor receptor autocrine loop is necessary for Ras transformation of Rat intestinal epithelial cells, J. Biol. Chem. 272 (1997) 18926–18931.
[19] A. Schulze, K. Lehmann, H.B.J. Jefferies, M. McMahon, J. Downward, Analysis of the transcriptional program induced by Raf in epithelial cells, Genes Dev. 15 (2001) 981–994.
[20] P.J. Robert, C.J. Der, Targeting the Raf-MEK-ERK mitogen-activated protein kinase cascade for the treatment of cancer, Oncogene 26 (2007) 3291–3310.
[21] M. Sibilia, A. Fleischmann, A. Behrens, L. Stingl, J. Carroll, F.M. Watt, J. Schlessinger, E.F. Wagner, The EGF receptor provides an essential survival signal for SOS-dependent skin tumor development, Cell 102 (2000) 211–220.
[22] R. Iwamoto, S. Yamazaki, M. Asakura, S. Takashima, H. Hasuwa, K. Miyado, S. Adachi, M. Kitakaze, K. Hashimoto, G. Raab, D. Nanba, S. Higashiyama, M. Hori, M. Klagsbrun, E. Mekada, Heparin-binding EGF-like growth factor and ErbB signaling is essential for heart function, Proc. Natl. Acad. Sci. USA 100 (2003) 3221–3226.
[23] C. Mitchell, M. Nivison, L.F. Jackson, R. Fox, D.C. Lee, J.S. Campbell, N. Fausto, Heparin-binding epidermal growth factor-like growth factor links hepatocyte priming with cell cycle progression during liver regeneration, J. Biol. Chem. 280 (2005) 2562–2568.
[24] N.C. Luetteke, T.H. Qiu, S.E. Fenton, K.L. Troyer, R.F. Riedel, A. Chang, D.C. Lee, Targeted inactivation of the EGF and amphiregulin genes reveals distinct roles for EGF receptor ligands in mouse mammary gland development, Development 126 (1999) 2739–2750.
[25] C. Berasain, E.R. Garcia-Trevijano, J. Castillo, E. Erroba, M. Santamaria, D.C. Lee, J. Prieto, M.A. Avila, Novel role for amphiregulin in protection from liver injury, J. Biol. Chem. 280 (2005) 19012–19020.
[26] K.L. Troyer, N.C. Luetteke, M.L. Saxon, T.H. Qiu, C.J. Xian, D.C. Lee, Growth retardation, duodenal lesions, and aberrant ileum architecture in triple null mice lacking EGF, amphiregulin, and TGF-α, Gastroenterology 121 (2001) 68–78.
[27] M. Wagner, C.K. Weber, F. Bressau, F.R. Greten, V. Stagge, M. Ebert, S.D. Leach, G. Adler, R.M. Schmid, Transgenic overexpression of amphiregulin induces a mitogenic response selectively in pancreatic duct cells, Gastroenterology 122 (2002) 1898–1912.
[28] N.C. Luetteke, T.H. Qiu, R.L. Peiffer, P. Oliver, O. Smithies, D.C. Lee, TGFα deficiency results in hair follicle and eye abnormalities in targeted and waved-1 mice, Cell 73 (1993) 263–278.
[29] G.B. Mann, K.J. Fowler, A. Gabriel, E.C. Nice, R.L. Williams, A.R. Dunn, Mice with a null mutation of the TGFα gene have abnormal skin architecture, wavy hair, and curly whiskers and often develop corneal inflammation, Cell 73 (1993) 249–261.
[30] L.F. Jackson, T.H. Qui, S.W. Sunnarborg, A. Chang, C. Zhang, C. Patterson, D.C. Lee, Defective valvulogenesis in HB-EGF and TACE-null mice is associated with aberrant BMP signaling, EMBO J. 22 (2003) 2704–2716.
[31] D. Lee, R.S. Pearsall, S. Das, S.K. Dey, V.L. Godfrey, D.W. Threadgill, Epiregulin is not essential for development of intestinal tumors but is required for protection from intestinal damage, Mol. Cell. Biol. 24 (2004) 8907–8916.

[32] K.K.L. Mak, S.Y. Chan, Epidermal growth factor as a biologic switch in hair growth cycle, J. Biol. Chem. 278 (2003) 26120–26126.
[33] M.R. Schneider, M. Dahlhoff, N. Herbach, I. Renner-Mueller, C. Dalke, O. Puk, J. Graw, R. Wanke, E. Wolf, Betacellulin overexpression in transgenic mice causes disproportionate growth, pulmonary hemorrhage syndrome, and complex eye pathology, Endocrinology 146 (2005) 5237–5246.
[34] F. Morigillo, H.Y. Lee, Resistance to epidermal growth factor receptor-targeted therapy, Drug Resist. Updat. 8 (2005) 298–310.

THE JOURNAL OF BIOLOGICAL CHEMISTRY VOL. 283, NO. 35, pp. 24234–24244, August 29, 2008

Interaction of Scaffolding Adaptor Protein Gab1 with Tyrosine Phosphatase SHP2 Negatively Regulates IGF-I-dependent Myogenic Differentiation via the ERK1/2 Signaling Pathway*[S]

Received for publication, May 21, 2008, and in revised form, June 18, 2008 Published, JBC Papers in Press, June 23, 2008, DOI 10.1074/jbc.M803907200

Tatsuya Koyama[‡§1], Yoshikazu Nakaoka[‡¶1,2], Yasushi Fujio[‖], Hisao Hirota[¶†], Keigo Nishida[**], Shoko Sugiyama[¶], Kitaro Okamoto[¶], Keiko Yamauchi-Takihara[¶], Michihiro Yoshimura[§], Seibu Mochizuki[§], Masatsugu Hori[¶], Toshio Hirano[‡‡], and Naoki Mochizuki[‡]**

From the [‡]Department of Structural Analysis, National Cardiovascular Center Research Institute, 5-7-1, Fujishirodai, Suita, Osaka, 565-8565, the [¶]Department of Cardiovascular Medicine, Osaka University Graduate School of Medicine, 2-2, Yamadaoka, Suita, Osaka, 565-0871, the [‖]Department of Clinical Pharmacology and Pharmacogenomics, Osaka University Graduate School of Pharmaceutical Sciences, 1-6, Yamadaoka, Suita, Osaka, 565-0871, the [**]Laboratory for Cytokine Signaling, RIKEN Research Center for Allergy and Immunology, 1-7-22, Suehiro-cho, Tsurumi-ku, Yokohama City, Kanagawa, 230-0045, the [§]Division of Cardiology, Department of Internal Medicine, The Jikei University School of Medicine, 3-25-8, Nishi-Shinbashi, Minato-ku, Tokyo, 105-8461, and the [‡‡]Laboratory of Developmental Immunology, Osaka University Graduate School of Frontier Biosciences and Graduate School of Medicine, 2-2, Yamadaoka, Suita, Osaka, 565-0871, Japan

Grb2-associated binder 1 (Gab1) coordinates various receptor tyrosine kinase signaling pathways. Although skeletal muscle differentiation is regulated by some growth factors, it remains elusive whether Gab1 coordinates myogenic signals. Here, we examined the molecular mechanism of insulin-like growth factor-I (IGF-I)-mediated myogenic differentiation, focusing on Gab1 and its downstream signaling. Gab1 underwent tyrosine phosphorylation and subsequent complex formation with protein-tyrosine phosphatase SHP2 upon IGF-I stimulation in C2C12 myoblasts. On the other hand, Gab1 constitutively associated with phosphatidylinositol 3-kinase regulatory subunit p85. To delineate the role of Gab1 in IGF-I-dependent signaling, we examined the effect of adenovirus-mediated forced expression of wild-type Gab1 ($Gab1^{WT}$), mutated Gab1 that is unable to bind SHP2 ($Gab1^{\Delta SHP2}$), or mutated Gab1 that is unable to bind p85 ($Gab1^{\Delta p85}$), on the differentiation of C2C12 myoblasts. IGF-I-induced myogenic differentiation was enhanced in myoblasts overexpressing $Gab1^{\Delta SHP2}$, but inhibited in those overexpressing either $Gab1^{WT}$ or $Gab1^{\Delta p85}$. Conversely, IGF-I-induced extracellular signal-regulated kinase 1/2 (ERK1/2) activation was significantly repressed in myoblasts overexpressing $Gab1^{\Delta SHP2}$ but enhanced in those overexpressing either $Gab1^{WT}$ or $Gab1^{\Delta p85}$. Furthermore, small interference RNA-mediated Gab1 knockdown enhanced myogenic differentiation. Overexpression of catalytic-inactive SHP2 modulated IGF-I-induced myogenic differentiation and ERK1/2 activation similarly to that of $Gab1^{\Delta SHP2}$, suggesting that Gab1-SHP2 complex inhibits IGF-I-dependent myogenesis through ERK1/2. Consistently, the blockade of ERK1/2 pathway reversed the inhibitory effect of $Gab1^{WT}$ overexpression on myogenic differentiation, and constitutive activation of the ERK1/2 pathway suppressed the enhanced myogenic differentiation by overexpression of $Gab1^{\Delta SHP2}$. Collectively, these data suggest that the Gab1-SHP2-ERK1/2 signaling pathway comprises an inhibitory axis for IGF-I-dependent myogenic differentiation.

Skeletal muscle differentiation is a multistep process in which multipotent mesodermal cells give rise to myoblasts that subsequently withdraw from the cell cycle and differentiate into multinucleated myotubes. Most skeletal muscle cell lines from rodents proliferate in high serum conditions containing various mitogens, and post-confluent cells spontaneously differentiate after several days in low serum conditions (1, 2). Among various growth factors, the insulin-like growth factors (IGFs),[3] includ-

* This work was supported by grants from the Ministry of Education, Science, Sports and Culture of Japan (to Y. N., K. Y.-T., and N. M.); the Ministry of Health, Labour, and Welfare of Japan (to N. M.); the Program for the Promotion of Fundamental Studies in Health Sciences of the National Institute of Biomedical Innovation (to N. M.); the Takeda Medical Research Foundation (to N. M.); The Uehara Memorial Foundation (to Y. N.); the Japan Heart Foundation Young Investigator's Research Grant (to Y. N.); the Suzuken Memorial Foundation (to Y. N.); the Astellas Foundation for Research on Metabolic Disorders (to Y. N.); the Senri Life Science Foundation (to Y. N.); and the Miyata Cardiology Research Promotion Funds (to Y. N.). The costs of publication of this article were defrayed in part by the payment of page charges. This article must therefore be hereby marked "*advertisement*" in accordance with 18 U.S.C. Section 1734 solely to indicate this fact.

[S] The on-line version of this article (available at http://www.jbc.org) contains supplemental text, references, and Figs. S1 and S2.

† Deceased on December 27, 2005.

[1] Both authors contributed equally to this work.

[2] To whom correspondence should be addressed: Dept. of Cardiovascular Medicine, Osaka University Graduate School of Medicine, Suita, Osaka 565-0871, Japan. Tel.: 81-6-6879-3835; Fax: 81-6-6879-3839; E-mail: ynakaoka@imed3.med.osaka-u.ac.jp.

[3] The abbreviations used are: IGF, insulin-like growth factor; Gab1, Grb2-associated binder 1; Gab2, Grb2-associated binder 2; WT, wild-type; PI3K, phosphatidylinositol 3-kinase; MAPK, mitogen-activated protein kinase; MEK1/2, MAPK/extracellular signal-regulated kinase kinase 1/2; ERK1/2, extracellular signal-regulated kinase 1/2; SH2, Src homology 2; SHP2, SH2-containing protein-tyrosine phosphatase 2; EGF, epidermal growth factor; VEGF, vascular endothelial growth factor; IRS-1, insulin receptor substrate-1; MHC, myosin heavy chain; DMEM, Dulbecco's modified Eagle's medium; FBS, fetal bovine serum; β-gal, β-galactosidase; HS, horse serum; FGF2, fibroblast growth factor 2; IP, immunoprecipitation; ANOVA, analysis of variance; siRNA, small interference RNA; RNAi, RNA interference.

ing IGF-I and IGF-II, have been reported to be quite unique in that they stimulate both proliferation and differentiation of muscle cells in culture (3, 4). IGF-I receptor belongs to the receptor tyrosine kinase family and utilizes two major cytoplasmic signaling pathways, namely the phosphatidylinositol 3-kinase (PI3K) cascade and mitogen-activated protein kinase (MAPK) cascade, which consists of Raf-MAPK/extracellular signal-regulated kinase (ERK)-kinase1/2 (MEK1/2)-ERK1/2 (5). PI3K is one of the primary signaling molecules promoting skeletal muscle differentiation, as demonstrated by pharmacological and genetic methods (3, 6, 7). On the other hand, activation of Raf-MEK1/2-ERK1/2 MAPK cascade has been reported to have inhibitory effects on the myogenic differentiation induced by insulin or IGFs (3, 8–10).

Grb2-associated binder 1 (Gab1) belongs to the scaffolding adaptor protein family. Gab1 has an N-terminal pleckstrin homology domain, as well as multiple tyrosine-based motifs and proline-rich sequences, which are potential binding sites for various Src homology 2 (SH2) domains and Src homology 3 domains, respectively. Gab1 undergoes tyrosine phosphorylation upon stimulation with various growth factors, cytokines, G protein-coupled receptor agonists, and various immuno-antigens (11,12). Tyrosine-phosphorylated Gab1 provides docking sites for multiple SH2 domain-containing signaling molecules, such as SH2-containing protein-tyrosine phosphatase SHP2, PI3K regulatory subunit p85, phospholipase C-γ, Crk, and Ras GTPase-activating protein (11–17). Among these binding partners, SHP2, a ubiquitously expressed protein-tyrosine phosphatase, has crucial roles for receptor tyrosine kinase-dependent activation of ERK1/2 in association with Gab1 (18, 19). The functional significance of Gab1-SHP2 interaction has been extensively studied using the Gab1 mutant that is unable to bind SHP2. This Gab1 mutant is defective in delivering signals for hepatocyte growth factor-c-Met-dependent morphogenesis, epidermal growth factor (EGF)-dependent epidermal proliferation, and leukemia inhibitory factor-gp130-dependent cardiomyocyte hypertrophy (20–23). These findings underscore the importance of Gab1-SHP2 interaction and strongly suggest that the primary role of Gab1 might be to recruit SHP2 (24). On the other hand, it has been reported that Gab1 also regulates the PI3K-AKT signaling pathway through association with p85 downstream of various growth factors (25–29). Gab1 has been reported to be required for both EGF-dependent activation of PI3K-AKT signaling pathway and migration of keratinocytes (28–30). In addition, Gab1 plays a key role for vascular endothelial growth factor-dependent activation of the PI3K signaling pathway and is required for endothelial cell migration and capillary formation (25, 27).

Gab1knockout (Gab1KO) mice died *in utero* and displayed developmental defects in the heart, placenta, liver, skin, and skeletal muscle (31, 32). Furthermore, Gab1KO mice displayed reduced and delayed migration of muscle progenitor cells into the limbs and diaphragm, resulting in the immature formation of limb muscles. These data suggest that Gab1 might have a key role in skeletal muscle development (32). We created cardiomyocyte-specific Gab1/Gab2 double knock-out mice and revealed that Gab1 and Gab2 play redundant, but essential roles in postnatal maintenance of cardiac function via the neuregulin-1/ErbB signaling pathway (33). In addition, liver-specific Gab1 knock-out mice displayed enhanced hepatic insulin sensitivity with reduced glycemia and improved glucose tolerance as a result of insufficient insulin-elicited activation of ERK1/2 (34). However, it remains elusive whether Gab1 has a specific role in skeletal muscle differentiation. In this study, we demonstrate for the first time that Gab1-SHP2 interaction exerts an inhibitory effect on IGF-I-induced myogenic differentiation via activation of the ERK1/2 signaling pathway.

EXPERIMENTAL PROCEDURES

Reagents and Antibodies—Anti-phospho-p44/42 ERK1/2 (Thr-202/Tyr-204), anti-phospho-AKT (Thr-308), anti-ERK1/2, and anti-AKT antibodies were purchased from Cell Signaling Technology. Anti-Gab1 and anti-Gab2 sera for immunoprecipitation were described previously (15, 16, 22). The antibodies against the following molecules used for immunoblotting, Gab1, Gab2, insulin receptor substrate-1 (IRS-1), and p85 PI3K were from Millipore; PY99, SHP2, MEK1, and myogenin were from Santa Cruz Biotechnology. Anti-myosin heavy chain (MHC) monoclonal antibody (MF20) was purchased from the Developmental Hybridoma Bank (Dr. D. A. Fischman, University of Iowa, Iowa City, IA). Hoechst 33342 nuclear dye was from Sigma. Horseradish peroxidase-conjugated anti-mouse and anti-rabbit antibodies were from GE Health Science. U0126 was from Promega (Madison, WI). Serum and cell culture reagents were from Invitrogen. Human recombinant IGF-I was kindly provided by Astellas Pharmaceuticals.

Adenovirus Vector Construction—The generation of adenovirus vectors expressing human Gab1^{WT} and Gab1$^{\Delta SHP2}$ (mutated on the two tyrosine residues responsible for binding with SHP2) were described previously (22). In this study, we constructed the adenovirus vectors expressing Gab1$^{\Delta p85}$, which can't bind with p85 due to the substitution of tyrosine residues 447, 472, and 589 of human Gab1, corresponding to the *YXXM* motifs, to phenylalanines by PCR-based mutagenesis described previously (35). Substitution of these tyrosine residues by phenylalanine renders the molecule incapable of binding with p85. We also constructed adenovirus vectors expressing wild-type SHP2 (SHP2^{WT}) and phosphatase-inactive SHP2 (SHP2$^{C/S}$) using the plasmid vectors described previously (15). For adenovirus production, the sequence encoding Gab1$^{\Delta p85}$, SHP2^{WT}, or SHP2$^{C/S}$ was subcloned into the shuttle plasmid pACCMVpLpA. Recombinant adenoviruses were then obtained according to the homologous recombination system described elsewhere (36). The adenovirus vectors expressing constitutive-active MEK1 and dominant-negative MEK1 were kindly provided by Dr. S. Kawashima (Kobe University) and described previously (37). The construction of adenovirus vector expressing human Gab2$^{\Delta SHP2}$, which can't bind with SHP2, is described in the supplemental data.

Cell Culture, Stimulation, and Adenoviral Infection—C2C12 murine myoblast cells were maintained as subconfluent monolayers in Dulbecco's modified Eagle's medium (DMEM) containing 4.5 g/liter glucose, 0.58 g/liter L-glutamine, 100 units/ml penicillin, and 100 μg/ml streptomycin supplemented with

20% fetal bovine serum (FBS). Before stimulation, cells were serum-starved overnight. Stimulations were performed using 80 ng/ml IGF-I for 10 min, unless otherwise indicated. For adenoviral infection of C2C12 myoblasts, subconfluent cells were cultured in DMEM with 20% FBS at a multiplicity of infection of 50 for 24 h. In the dual infection of adenovirus vectors, C2C12 cells were cultured in DMEM with 20% FBS with each virus at a multiplicity of infection of 30. Then, the myoblasts were serum-starved overnight and stimulated with or without IGF-I for the experiments examining ERK1/2 and AKT phosphorylation. Infection efficiency, determined by *lacZ* gene expression in cultured myoblasts, is consistently >90% with this method. Adenovirus vector expressing β-galactosidase (β-gal) was used as a control. For the induction of myogenic differentiation, cultured medium was switched from DMEM containing 20% FBS to DMEM containing 2% horse serum (HS) or 80 ng/ml IGF-I, when cell density reached confluency. The differentiation medium containing 2% HS was exchanged every other day, and that containing IGF-I was exchanged every day.

Cell Lysis, Immunoprecipitations, and Immunoblotting—Cells were scraped off in lysis buffer containing 20 mM Tris (pH 7.4), 150 mM NaCl, 3 mM EDTA, 1% Nonidet P-40, 2 mM sodium orthovanadate, and protease inhibitor mixture Complete (Roche Applied Science). Cell lysates were collected form confluent 6-cm dishes and precleared by 15,000 × *g* centrifugation for 15 min. For immunoprecipitation, the cleared lysates of 500 μl containing 1 mg of protein, were rotationally incubated with 1 μl of anti-Gab1 antiserum, or 1.2 μg of SHP2 antibody, or 5 μl of p85 antibody, or 10 μl of IRS-1 antibody and with 20 μl of protein A-Sepharose (GE Healthcare) overnight at 4 °C. The antigen-antibody complexes were collected by centrifugation, washed three times with lysis buffer without protease inhibitor mixture, and boiled in standard electrophoresis sample buffer. All the proteins immunoprecipitated were then resolved by SDS-PAGE and subjected to immunoblotting using a standard procedure. Blots were developed using ECL system (GE Healthcare). For direct immunoblotting analyses, the crude cell lysates were collected from 3.5-cm dishes and subjected to 15,000 × *g* centrifugation. The precleared lysates containing 30 μg of protein were loaded in each lane for immunoblotting.

Immunocytochemistry—Cells cultured on 3.5-cm collagen type I-coated plastic dishes (Iwaki Asahi Glass Co.) were fixed with 2% formaldehyde in phosphate-buffered saline and permeabilized with 0.1% Triton X-100 for 10 min. Cells were blocked with phosphate-buffered saline containing 1% bovine serum albumin for 1 h and incubated with anti-MHC antibody (MF20), followed by incubation with Alexa 488-labeled goat anti-mouse secondary antibody (Molecular Probes). Cells were post-stained with Hoechst 33342 nuclear dye and viewed by fluorescence microscopy.

siRNA-mediated Protein Knockdown—Stealth Select small interfering RNAs (siRNAs) targeted to murine Gab1 (#1, MSS204497; #2, MSS204499) and siRNA duplex with irrelevant sequences (Stealth™ RNAi negative control) as a control were purchased from Invitrogen. Stealth siRNAs targeted to murine SHP2 were purchased from Invitrogen. and the detailed sequences are described in the supplemental data. C2C12 myoblasts were transfected with 10 nM siRNA duplexes using Lipofectamine™ RNAiMAX reagent according to the manufacturer's instructions for reverse transfection. Briefly, C2C12 myoblasts (1.5×10^5 cells per each dish) were diluted in 860 μl of DMEM containing 20% FBS and plated on 3.5-cm collagen type I-coated plastic dishes. To each dish, 140 μl of RNAi duplex-Lipofectamine™ RNAiMAX complex diluted in Opti-MEM I medium was added. After incubation for 72 h, the cells were used for the experiments.

Statistics—All data are expressed as mean ± S.D. Differences among multiple groups were compared by one-way ANOVA followed by a post hoc comparison tested with Scheffe's method. Values of $p < 0.05$ were considered significant.

RESULTS

Gab1 Undergoes Tyrosine Phosphorylation and Subsequently Associates with SHP2 upon IGF-I Stimulation in C2C12 Myoblasts—We examined the effect of IGF-I on tyrosine-phosphorylation of Gab1 and its association with SH2 domain-containing signaling molecules in C2C12 myoblasts. IGF-I indeed induced tyrosine phosphorylation of Gab1 and subsequent association of Gab1 with SHP2 in C2C12 myoblasts (Fig. 1*A*, *left panel*). Furthermore, SHP2 was also tyrosine-phosphorylated and associated with Gab1 after stimulation with IGF-I (Fig. 1*A*, *right panel*). On the other hand, Gab1 constitutively associated with p85 both before and after IGF-I stimulation (Fig. 1*A*, *left panel*). In the IGF-I-dependent signaling pathway, IRS-1 has been reported to be a major binding partner of p85 and essential for IGF-I-dependent PI3K-AKT signaling in skeletal muscle cells (38). Consistently, IRS-1 underwent strong tyrosine phosphorylation after stimulation with IGF-I in C2C12 myoblasts. In clear contrast to Gab1, IRS-1 associated with p85 in a manner dependent on IGF-I stimulation (Fig. 1*B*). In addition, we could not detect the complex formation of IRS-1 with SHP2 either before or after stimulation with IGF-I (Fig. 1*B*). These results demonstrate that IGF-I induces tyrosine phosphorylation of Gab1, leading to complex formation of Gab1 with SHP2 in C2C12 myoblasts.

IGF-I-induced Tyrosine Phosphorylation of Gab1 and Association of Gab1 with SH2 Domain-containing Molecules in the C2C12 Myoblasts Infected with Adenovirus Vectors—IGFs have been reported to stimulate both proliferation and differentiation of cultured skeletal muscle cells (3, 4). The effect of IGF-I on the proliferation of myoblasts has been reported to be attributed mainly to ERK1/2 pathway (3). In the present study, we tried to reveal the role of Gab1 in IGF-I-dependent differentiation from myoblasts into myotubes. To discern the role of Gab1-SHP2 interaction from that of Gab1-p85 interaction in IGF-I-dependent differentiation, we used recombinant adenovirus vectors carrying β-gal (control), $Gab1^{WT}$, or $Gab1^{\Delta SHP2}$ as described previously (22) and created an adenovirus vector overexpressing $Gab1^{\Delta p85}$. We examined tyrosine phosphorylation of Gab1 upon stimulation with IGF-I in myoblasts overexpressing β-gal, $Gab1^{WT}$, $Gab1^{\Delta SHP2}$, or $Gab1^{\Delta p85}$. As shown in Fig. 2*A*, tyrosine phosphorylation of Gab1 and the amount of co-immunoprecipitated SHP2 with Gab1 were increased after stimulation with IGF-I in control myoblasts expressing β-gal. On the other hand, tyrosine phosphorylation of Gab1 in the

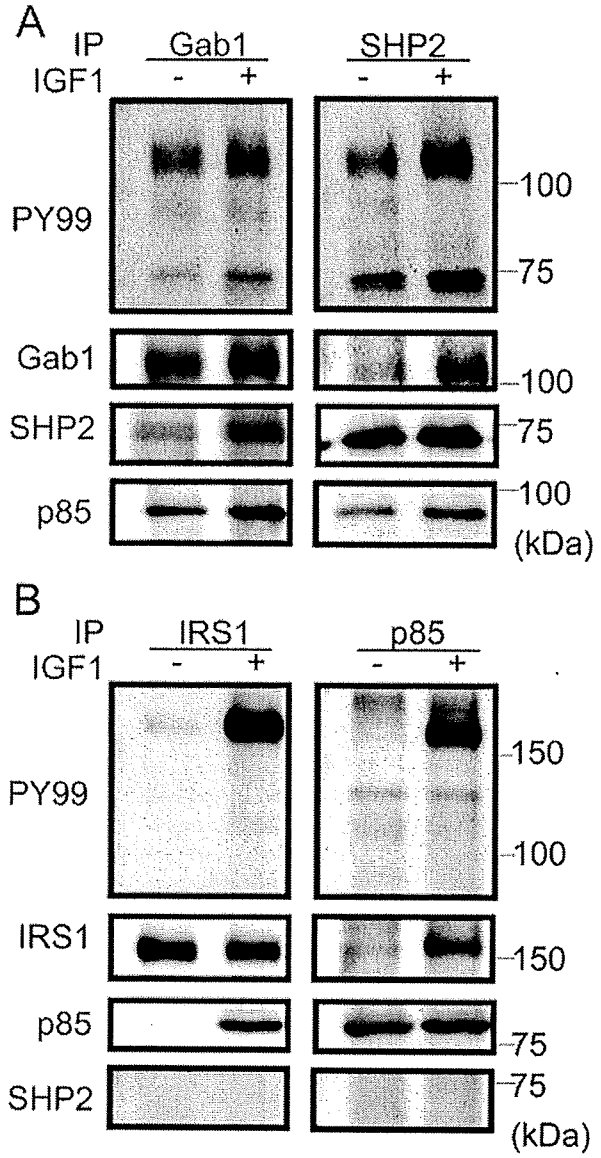

FIGURE 1. **IGF-I induces tyrosine phosphorylation of Gab1 and complex formation of Gab1 with SHP2 in C2C12 myoblasts.** Serum-starved C2C12 myoblast cells were stimulated with 80 ng/ml IGF-I for 10 min, and cell lysates of 500 μl harvested from 6 cm dishes were subjected to immunoprecipitation analysis with anti-Gab1 serum (*A, left panel*), anti-SHP2 antibody (*A, right panel*), anti-IRS-1 antibody (*B, left panel*), or anti-p85 antibody (*B, right panel*). Immunoprecipitates were subjected to SDS-PAGE followed by immunoblot analysis with anti-phosphotyrosine antibody (PY99). The same membrane was reprobed with the antibodies indicated at the *left* (anti-Gab1, anti-SHP2, and anti-p85 antibodies). *A*, both Gab1 and SHP2 were tyrosine-phosphorylated and co-immunoprecipitated with each other in an IGF-I-dependent manner. On the other hand, the association of Gab1 with p85 did not change either before or after IGF-I treatment. *B*, upon stimulation with IGF-I, IRS-1 became strongly tyrosine-phosphorylated and co-immunoprecipitated with p85. However, co-immunoprecipitation of IRS-1 with SHP2 was not detected. Experiments were repeated three times with similar results.

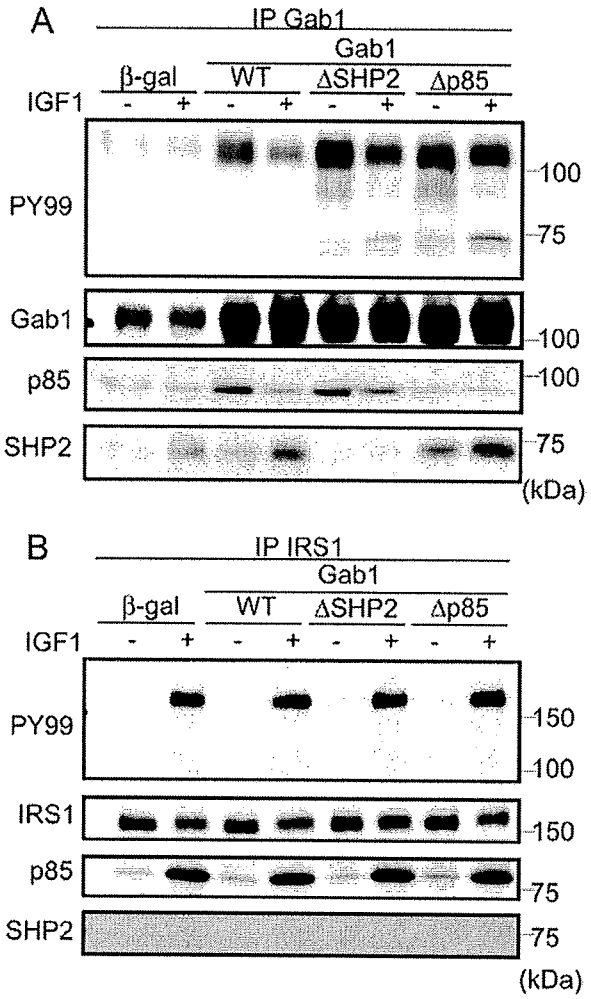

FIGURE 2. **Overexpression of Gab1$^{\Delta SHP2}$ or Gab1$^{\Delta p85}$ specifically perturbs the IGF-I-dependent molecular association of Gab1 with SHP2 or p85, respectively.** C2C12 myoblasts were infected with adenovirus vectors expressing β-gal, Gab1^{WT}, Gab1$^{\Delta SHP2}$, or Gab1$^{\Delta p85}$. Serum-starved C2C12 cells were stimulated with vehicle (−) or IGF-I for 10 min, and cell lysates of 500 μl were collected from 6-cm dishes. Cell lysates were subjected to immunoprecipitation with anti-Gab1 serum (*A*) or with anti-IRS-1 antibody (*B*), followed by immunoblotting with anti-phosphotyrosine antibody (PY99). *A*, blots were reprobed with anti-Gab1, anti-p85, and anti-SHP2 antibodies. *B*, blots were reprobed with anti-IRS-1, anti-p85, and anti-SHP2 antibodies. Experiments were repeated three times with similar results.

myoblasts overexpressing Gab1^{WT}, Gab1$^{\Delta SHP2}$, or Gab1$^{\Delta p85}$ increased much more at baseline compared with in those overexpressing β-gal. In these cells, tyrosine phosphorylation of Gab1 decreased after stimulation with IGF-I. The IGF-I-induced association of Gab1 with SHP2 increased in the C2C12 myoblasts overexpressing Gab1^{WT}, or Gab1$^{\Delta p85}$ compared with those overexpressing β-gal, but was almost abrogated in those overexpressing Gab1$^{\Delta SHP2}$ (Fig. 2*A*). The co-immunoprecipitation of Gab1 with p85 was increased in cells expressing Gab1^{WT} or Gab1$^{\Delta SHP2}$ compared with those expressing β-gal, but was almost abrogated in those expressing Gab1$^{\Delta p85}$ at the baseline. The association of Gab1 with p85 decreased in response to IGF-I in the cells overexpressing Gab1^{WT} or Gab1$^{\Delta SHP2}$ (Fig. 2*A*). We observed much more dissociation of p85 from Gab1 in myoblasts overexpressing Gab1^{WT} compared with those overexpressing Gab1$^{\Delta SHP2}$, which might be attributed to the increased activation of SHP2. Presumably, SHP2 dephosphorylates the tyrosine residues for p85 binding site of Gab1 consistent with the previous report on EGF-dependent signaling (39). These data demonstrate that overexpression of

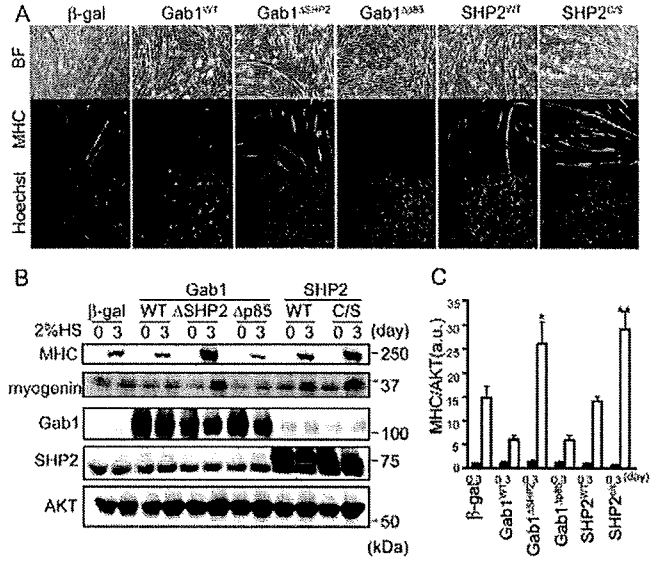

FIGURE 3. **Myogenic differentiation in a low serum condition is negatively regulated by Gab1-SHP2 complex through activating phosphatase activity of SHP2 in C2C12 myoblasts.** *A*, immunocytochemical analysis of C2C12 myoblasts using anti-MHC antibody. C2C12 myoblasts were infected with adenovirus vectors expressing β-galactosidase (β-gal), $Gab1^{WT}$, $Gab1^{\Delta SHP2}$, $Gab1^{P85}$, $SHP2^{WT}$, or $SHP2^{C/S}$ and induced into myogenic differentiation by switching the growth medium containing 20% fetal bovine serum to the differentiation medium containing 2% horse serum. On the third day after induction, cells were immunostained with anti-MHC antibody and post-stained with nuclear dye Hoechst 33342. *BF*, bright field image. Experiments were repeated three times with similar results. *B*, Western blot analysis of myoblasts infected with indicated adenovirus vectors before and after low serum-induced myogenic induction for 3 days. Cell lysates were subjected to Western blot analysis using anti-MHC and anti-myogenin antibodies. The membrane was stripped and reprobed with anti-Gab1 or anti-SHP2 antibodies for confirmation of adenoviral overexpression of Gab1 or SHP2. AKT expression was also examined for loading control. *C*, the relative expression level of MHC was quantified by normalizing the expression of MHC by that of AKT. Values are expressed as means ± S.D. of three independent experiments (*, $p < 0.05$ or **, $p < 0.01$ compared with control cells expressing β-gal on the same day after myogenic induction, by one-way ANOVA). *a.u.*, arbitrary unit(s).

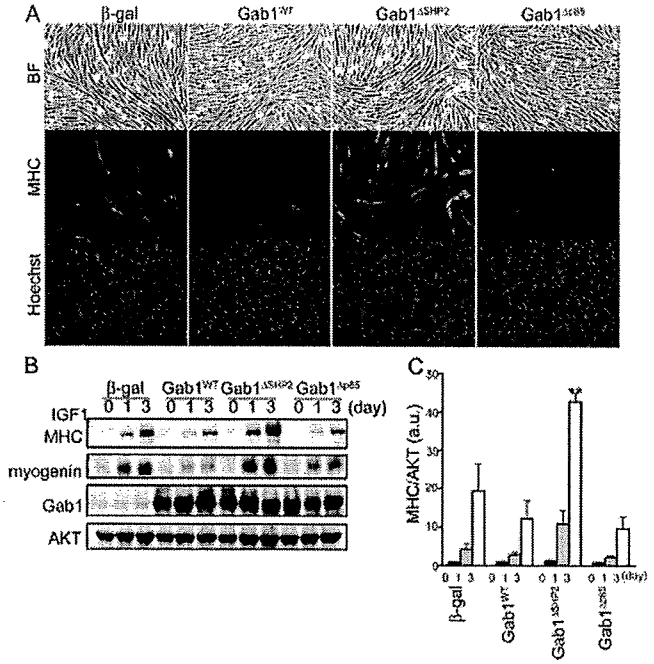

FIGURE 4. **IGF-I-induced myogenic differentiation is negatively regulated by interaction of Gab1 with SHP2 in C2C12 myoblasts.** *A*, immunocytochemical analysis of C2C12 myoblasts overexpressing various Gab1 proteins. C2C12 myoblasts infected with adenovirus vectors overexpressing β-gal, $Gab1^{WT}$, $Gab1^{\Delta SHP2}$, or $Gab1^{\Delta p85}$ (as indicated at the top), were cultured in differentiation medium containing IGF-I. On the third day after exposure to the differentiation medium containing IGF-I, cells were immunostained with anti-MHC antibody and post-stained with Hoechst 33342 nuclear dye. Experiments were repeated three times with similar results. *B*, cell lysates were collected from C2C12 cells overexpressing β-gal, $Gab1^{WT}$, $Gab1^{\Delta SHP2}$, or $Gab1^{\Delta p85}$ at the indicated time after cultivation in the differentiation medium containing IGF-I. Cell lysates were subjected to Western blot analysis for analyzing the expression of MHC and myogenin. The membrane was reprobed with anti-Gab1 antibody for confirmation of adenoviral overexpression of Gab1. AKT was also examined as a loading control. *C*, the relative expression level of MHC was quantified by normalizing the expression of MHC by that of AKT. Values are shown as mean ± S.D. of three independent experiments (**, $p < 0.01$ compared with control cells expressing β-gal on the same day after myogenic induction, by one-way ANOVA). *a.u.*, arbitrary unit(s).

$Gab1^{\Delta SHP2}$ or $Gab1^{\Delta p85}$ sufficiently suppresses the association of Gab1 with SHP2 or p85, respectively.

On the other hand, tyrosine phosphorylation of IRS-1 and interaction between IRS-1 and p85 were comparable among the four groups of cells after stimulation with IGF-I (Fig. 2*B*). Thus, these findings indicate that overexpression of $Gab1^{\Delta SHP2}$ or $Gab1^{\Delta p85}$ specifically perturbs the IGF-I-dependent interaction of Gab1 with SHP2 or p85, respectively.

Myogenic Differentiation Induced by a Low Serum Condition Is Negatively Regulated by Gab1-SHP2 Complex through Activating SHP2 in C2C12 Myoblasts—C2C12 myoblasts undergo myogenic differentiation under a low-serum condition such as 2% HS (1, 2). Therefore, we examined the effects of overexpression of $Gab1^{WT}$, $Gab1^{\Delta SHP2}$, or $Gab1^{\Delta p85}$, on myogenic differentiation under low serum condition. After infection with adenovirus vectors for 24 h, confluent C2C12 myoblasts were cultured in the DMEM containing 2% HS. On the third day after induction of myogenic differentiation, cells were immunostained with anti-MHC antibody for evaluation of myogenic differentiation. The extent of myogenic differentiation was enhanced in myoblasts overexpressing $Gab1^{\Delta SHP2}$, but inhibited in myoblasts overexpressing either $Gab1^{WT}$ or $Gab1^{\Delta p85}$, compared with myoblasts infected with control adenovirus vector expressing β-gal (Fig. 3*A*). Western blot analysis also revealed that the expression of MHC was significantly increased by the overexpression of $Gab1^{\Delta SHP2}$, but seemed to be repressed by the overexpression either $Gab1^{WT}$ or $Gab1^{\Delta p85}$, compared with control (Fig. 3, *B* and *C*). These findings indicate that Gab1-SHP2 interaction exerts an inhibitory effect on myogenic differentiation induced by a low serum condition.

Gab1-SHP2 complex formation has been reported to result in an increase of phosphatase activity of SHP2 upon stimulation with EGF (20, 21, 24). To confirm the requirement of catalytic activity of SHP2 for inhibition of myogenesis, we created adenovirus vectors expressing wild-type SHP2 ($SHP2^{WT}$) and phosphatase-inactive SHP2 ($SHP2^{C/S}$). After infection with adenovirus vectors for 24 h, confluent C2C12 myoblasts were cultured in the DMEM containing 2% HS. The extent of myogenic differentiation determined by immunocytochemistry was enhanced in myoblasts overexpressing $SHP2^{C/S}$ compared with myoblasts overexpressing β-gal or $SHP2^{WT}$ (Fig. 3*A*). Consistently, Western blot analysis showed that overexpression of $SHP2^{C/S}$ in C2C12 cells induced significant increase of MHC

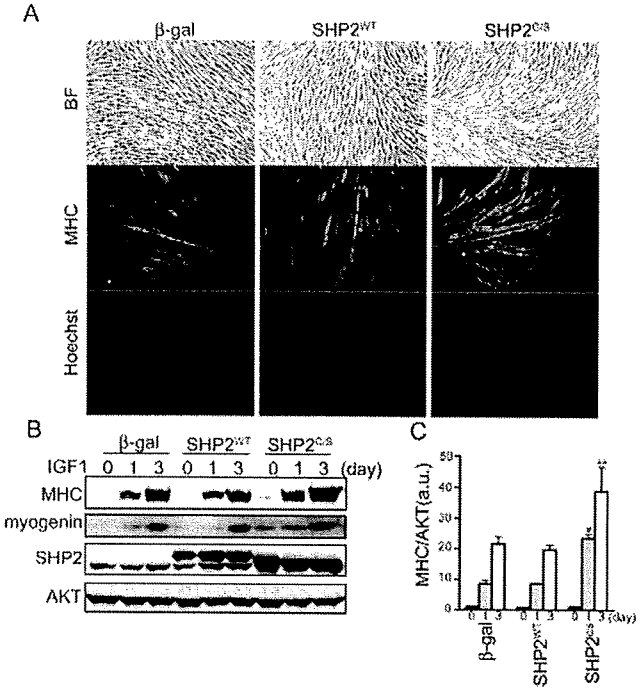

FIGURE 5. **SHP2 phosphatase activity is required for inhibition of myogenic differentiation.** *A*, C2C12 myoblasts overexpressing β-gal, $SHP2^{WT}$, or $SHP2^{C/S}$ were cultured in differentiation medium containing IGF-I. On the third day after exposure to the differentiation medium, cells were immunostained with anti-MHC antibody and post-stained with Hoechst 33342 nuclear dye. Myogenic differentiation was enhanced in myoblasts overexpressing $SHP2^{C/S}$ compared with myoblasts overexpressing β-gal and $SHP2^{WT}$. Experiments were repeated three times with similar results. *B*, cell lysates were collected from C2C12 cells overexpressing β-gal, $SHP2^{WT}$, or $SHP2^{C/S}$ at the indicated time after cultivation in the differentiation medium containing IGF-I. Cell lysates were subjected to Western blot analysis for analyzing the expression of MHC and myogenin. The membrane was reprobed with anti-SHP2 antibody for confirmation of adenoviral overexpression of SHP2. AKT was examined as a loading control. *C*, the relative expression level of MHC was quantified by normalizing the expression of MHC by that of AKT. Values are shown as means ± S.D. (*, $p < 0.05$ or **, $p < 0.01$ compared with control cells expressing β-gal on the same day after myogenic induction, by one-way ANOVA). *a.u.*, arbitrary unit(s).

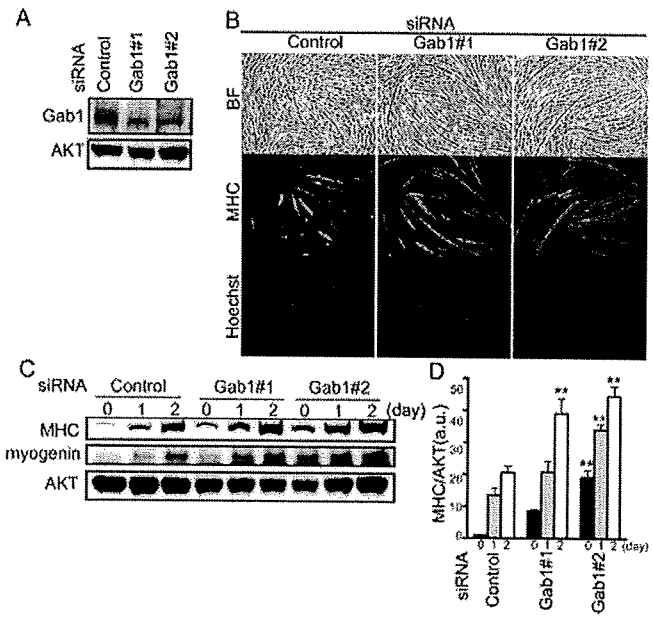

FIGURE 6. **siRNA-mediated Gab1 knockdown enhances myogenic differentiation.** *A*, C2C12 myoblasts were transfected with control siRNA (control) or with two independent siRNAs targeting different sequences of Gab1 (Gab1#1 and Gab1#2) for 72 h. Cell lysates were subjected to Western blot analysis. AKT was also checked as a loading control. *B*, C2C12 myoblasts were transfected with siRNAs as described in Fig. 6*A*. On the third day after transfection, the medium was changed from growth medium containing 20% FBS to differentiation medium containing 80 ng/ml IGF-I. Cells were cultured in the presence of IGF-I for 2 days. Cells were immunostained with anti-MHC antibody and post-stained with Hoechst 33342 nuclear dye. Experiments were repeated three times with similar results. *C*, cell lysates were collected at the indicated time after induction of myogenic differentiation and subjected to Western blot analysis. On the first and second day after myogenic induction, the expression level of MHC and myogenin were increased in cells transfected with Gab1 siRNAs (#1 or #2) compared with control. AKT was examined as a loading control. *D*, the relative expression level of MHC was quantified by normalizing the expression of MHC by that of AKT. Values are shown as means ± S.D. (**, $p < 0.01$ compared with control cells on the same day after myogenic induction, by one-way ANOVA). *a.u.*, arbitrary unit(s).

expression, compared with control (Fig. 3, *B* and *C*). Taken together, these findings suggest that Gab1 exerts an inhibitory effect on myogenic differentiation of C2C12 myoblasts under low serum condition through association with SHP2 and increase of SHP2 catalytic activity.

IGF-I-induced Myogenic Differentiation Is Negatively Regulated by Gab1-SHP2 Complex through Increasing Catalytic Activity of SHP2 in C2C12 Myoblasts—The IGF family, including IGF-I and -II, induces myogenic differentiation of myoblasts after myoblasts fully proliferate and become ready for differentiation (1–3). Therefore, we examined the effect of overexpression of various Gab1 proteins on the myogenic differentiation of C2C12 myoblasts cultured in IGF-I-containing differentiation medium. After infection with adenovirus vectors for 24 h, post-confluent C2C12 myoblasts were cultured in the DMEM containing 80 ng/ml IGF-I. On the third day after induction of myogenic differentiation, cells were immunostained with anti-MHC antibody. The extent of myogenic differentiation was enhanced in myoblasts overexpressing $Gab1^{\Delta SHP2}$ but inhibited in myoblasts overexpressing $Gab1^{WT}$ or $Gab1^{\Delta p85}$, compared with control (Fig. 4*A*). MHC expression was significantly increased in the myoblasts overexpressing $Gab1^{\Delta SHP2}$, although it seemed to be repressed in those overexpressing $Gab1^{WT}$ or $Gab1^{\Delta p85}$, compared with control (Fig. 4, *B* and *C*). Furthermore, the expression of myogenin was enhanced in myoblasts overexpressing $Gab1^{\Delta SHP2}$, but repressed in myoblasts overexpressing $Gab1^{WT}$ or $Gab1^{\Delta p85}$, compared with control (Fig. 4*B*). These data coincide with the results observed in the low serum condition, suggesting that Gab1-SHP2 complex has an inhibitory role in the IGF-I-induced myogenic differentiation.

Gab2, another Gab family protein, has been reported to complement the function of Gab1 in some signaling pathways such as EGF-dependent signaling (33, 40). To confirm the specific role of Gab1 in myogenic differentiation, we examined the effect of overexpression of $Gab2^{\Delta SHP2}$, the Gab2 mutant that cannot associate with SHP2 (41), on IGF-I-induced myogenic differentiation. The extent of myogenic differentiation was comparable between myoblasts overexpressing $Gab2^{\Delta SHP2}$ and those expressing β-gal (supplemental Fig. S1, *A* and *B*). We also confirmed that $Gab2^{\Delta SHP2}$ did not associate with SHP2 either before or after stimulation with IGF-I (supplemental Fig. S1*C*). These data suggested that IGF-I-induced myogenic differenti-

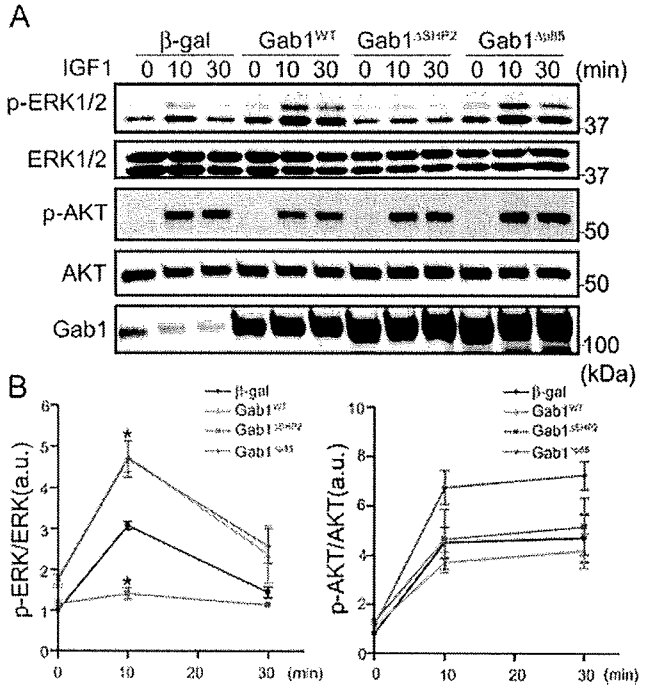

FIGURE 7. **IGF-I activates ERK1/2 via complex formation of Gab1 with SHP2 in C2C12 cells.** *A*, C2C12 cells infected with the indicated adenovirus vectors were serum-starved overnight and stimulated with IGF-I (80 ng/ml) for the indicated period. Cell lysates were collected at the indicated time and subjected to Western blot analysis using the antibodies indicated at the left. Expression level of Gab1 was almost comparable in the cells overexpressing $Gab1^{WT}$, $Gab1^{\Delta SHP2}$, or $Gab1^{\Delta p85}$. *B*, phosphorylation of ERK1/2 (*left*) and AKT (*right*) in *A* was quantified. Values are expressed as means ± S.D. of three independent experiments (*, $p < 0.05$, compared with control cells expressing β-gal at the same time after stimulation, by one-way ANOVA). *a.u.*, arbitrary unit(s).

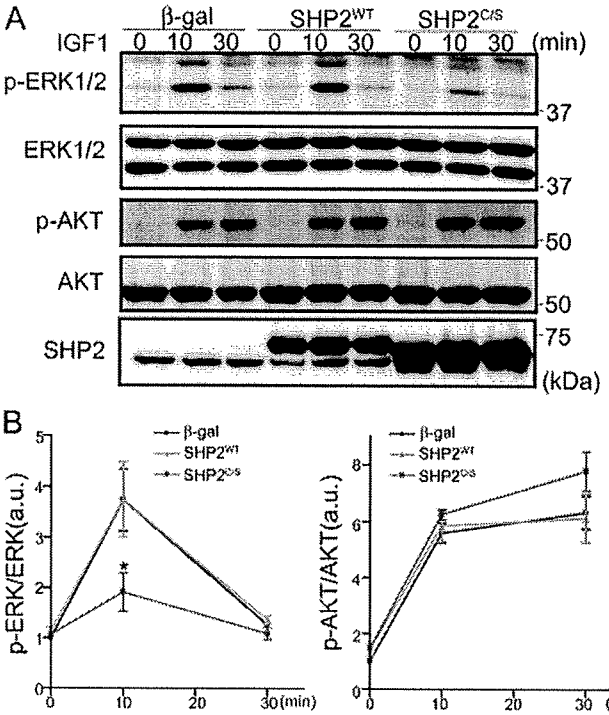

FIGURE 8. **IGF-I activates ERK1/2 via activation of SHP2 in C2C12 cells.** *A*, C2C12 cells infected with indicated adenovirus vectors were treated the same as in Fig. 7. Cell lysates were collected and subjected to Western blot analysis for analyzing ERK1/2 and AKT phosphorylation using the antibodies indicated at the left. Adenovirus-mediated overexpression of SHP2 was almost comparable in cells expressing $SHP2^{WT}$ or $SHP2^{C/S}$. *B*, phosphorylation of ERK1/2 (*left*) and AKT (*right*) in *A* was quantified. Values are shown as means ± S.D. from three independent experiments (*, $p < 0.05$ compared with control cells expressing β-gal at the same time after IGF-I stimulation, by one-way ANOVA). *a.u.*, arbitrary unit(s).

ation in C2C12 myoblasts might be regulated specifically by Gab1-SHP2 complex, but not by Gab2-SHP2 complex.

To confirm the requirement of SHP2 catalytic activity for the inhibitory effect of Gab1-SHP2 complex on myogenesis, C2C12 myoblasts were infected with adenovirus vectors expressing β-gal, $SHP2^{WT}$, or $SHP2^{C/S}$ and then treated with IGF-I-containing differentiation medium for the induction of myogenesis. Myogenic differentiation was enhanced in myoblasts overexpressing $SHP2^{C/S}$ compared with myoblasts overexpressing β-gal or $SHP2^{WT}$ (Fig. 5*A*). Western blot analysis also demonstrated that the MHC expression was significantly increased in the myoblasts overexpressing $SHP2^{C/S}$, but not in those overexpressing $SHP2^{WT}$, compared with control cells expressing β-gal (Fig. 5, *B* and *C*). Consistently, myogenin expression also seemed to be enhanced in those expressing $SHP2^{C/S}$, compared with myoblasts expressing β-gal or $SHP2^{WT}$ (Fig. 5*B*). These data indicate that Gab1-SHP2 complex has an inhibitory effect on IGF-I-elicited myogenic differentiation through activation of SHP2 in C2C12 myoblasts.

siRNA-mediated Knockdown of Gab1 Enhances Myogenic Differentiation in C2C12 Myoblasts—To examine the effect of Gab1 protein depletion in C2C12 myoblasts, we performed siRNA-mediated Gab1 knockdown. Gab1 protein expression was reduced by 80% in the myoblasts transfected with Gab1-targeted siRNAs compared with control cells (Fig. 6*A*). On the second day after induction of differentiation, cells were immunostained with anti-MHC antibody. The extent of myogenic differentiation was enhanced in myoblasts transfected with Gab1-targeted siRNAs compared with control (Fig. 6*B*). Consistently, Western blot analysis also revealed a significant increase of MHC expression in myoblasts transfected with Gab1-targeted siRNAs compared with control (Fig. 6, *C* and *D*). Furthermore, the expression of myogenin was increased in myoblasts transfected with Gab1-targeted siRNAs (Fig. 6*C*). These data coincide with the results obtained via overexpression experiments using adenovirus vectors and suggest that Gab1 has an inhibitory role in the IGF-I-induced myogenic differentiation.

Moreover, we performed siRNAs-mediated SHP2 knockdown in C2C12 myoblasts. SHP2 protein expression was reduced by 70% in the myoblasts transfected with SHP2-targeted siRNAs compared with control cells (supplemental Fig. S2*A*). On the contrary to the results obtained by Gab1-targeted siRNAs experiments, SHP2 knockdown inhibited proliferation of C2C12 myoblasts. Therefore, we could not evaluate the myogenic differentiation in C2C12 myoblasts transfected with SHP2-targeted siRNAs (supplemental Fig. S2*B*).

IGF-I-induced Activation of ERK1/2 Is Regulated by Gab1-SHP2 Complex through Activation of SHP2 in C2C12 Myoblasts—To elucidate a potential mechanism how Gab1 is involved in IGF-I-mediated myogenic differentiation of C2C12 myoblasts, we examined the effects of adenovirus-mediated overexpression of $Gab1^{WT}$, $Gab1^{\Delta SHP2}$, and $Gab1^{\Delta p85}$ on the

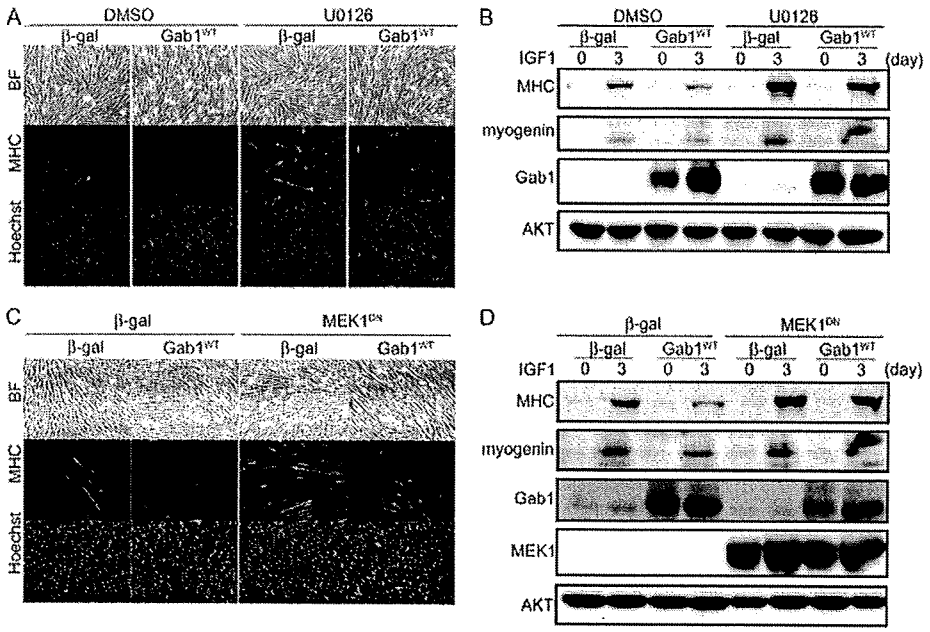

FIGURE 9. **ERK1/2 inhibition reverses the inhibitory effect of overexpression of Gab1^{WT} on IGF-I-induced myogenic differentiation.** *A*, C2C12 myoblasts were infected with adenovirus vectors overexpressing either β-gal or Gab1^{WT}. These cells were cultivated with or without a MEK1/2 inhibitor, U0126 (3 μM), under the differentiation medium containing 80 ng/ml IGF-I. On the third day after myogenic induction, the cells were immunostained with anti-MHC antibody and post-stained with Hoechst 33342 nuclear dye. Experiments were repeated three times with similar results. *B*, C2C12 cells overexpressing β-gal or Gab1^{WT} were cultured in the IGF-I-containing differentiation medium with or without U0126 (3 μM). Cell lysates were collected and subjected to Western blot analysis for analyzing the expression of MHC and myogenin. The membrane was reprobed with anti-Gab1 antibody for confirmation of adenoviral overexpression of Gab1. AKT was also checked as a loading control. *C*, C2C12 myoblasts were subjected to dual infection of adenovirus vectors expressing either β-gal or dominant-negative MEK1 (*MEK1^{DN}*) with Gab1^{WT}. On the third day after myogenic induction, the cells were immunostained with anti-MHC antibody and post-stained with Hoechst 33342 nuclear dye. Experiments were repeated three times with similar results. *D*, C2C12 myoblasts were subjected to dual infection of adenovirus vectors similarly to *B*. The cell lysates were collected and subjected to Western blot analysis for analyzing the expression of MHC and myogenin. The membrane was reprobed with anti-Gab1 and anti-MEK1 antibodies for confirmation of adenoviral overexpression of Gab1 and MEK1. AKT was also checked as a loading control. Experiments were repeated three times with similar results.

IGF-I-dependent signaling pathways downstream of Gab1. IGF-I induced activation of ERK1/2 and AKT in control myoblasts expressing β-gal. IGF-I-induced activation of ERK1/2 was significantly augmented in myoblasts overexpressing Gab1^{WT} or Gab1$^{\Delta p85}$ compared with control myoblasts expressing β-gal. On the other hand, activation of ERK1/2 was significantly reduced in myoblasts expressing Gab1$^{\Delta SHP2}$ (Fig. 7, *A* and *B*). On the other hand, activation of ERK1/2 was not changed in myoblasts expressing Gab2$^{\Delta SHP2}$ compared with control myoblasts expressing β-gal (supplemental Fig. S1*D*). These data indicate that Gab1 plays a critical role in IGF-I-induced ERK1/2 activation through interaction with SHP2 in C2C12 myoblasts.

IGF-I-induced AKT activation was almost comparable in myoblasts expressing β-gal, Gab1^{WT}, or Gab1$^{\Delta SHP2}$. On the contrary, activation of AKT seemed to be enhanced in cells overexpressing Gab1 $^{\Delta p85}$, compared with the other three groups (Fig. 7*B*). These data indicate that Gab1 might have a competitive role for sequestering p85 in the cytoplasm from other scaffolding adaptor proteins such as IRS-1.

To confirm the requirement of SHP2 activity for activation of ERK1/2 upon IGF-I stimulation, we examined the effects of adenovirus-mediated overexpression of SHP2^{WT} or SHP2$^{C/S}$ on ERK1/2 activation. IGF-I-induced activation of ERK1/2 was comparable in myoblasts overexpressing SHP2^{WT} and those expressing β-gal, but almost inhibited in cells overexpressing SHP2$^{C/S}$ compared with control (Fig. 8, *A* and *B*). On the other hand, activation of AKT was almost comparable among the three groups (Fig. 8, *A* and *B*). These findings indicate that SHP2 catalytic activity is indispensable for activation of ERK1/2 after stimulation with IGF-I in C2C12 myoblasts. Taken together, our findings indicate that IGF-I activates ERK1/2 via complex formation of Gab1 with SHP2 and activation of SHP2 in C2C12 myoblasts.

Gab1-SHP2-ERK1/2-signaling Pathway Is an Inhibitory Axis of IGF-I-dependent Myogenic Differentiation in C2C12 Myoblasts—It has been reported that ERK1/2 has an inhibitory role for myogenic differentiation of mesenchymal cells to date (3, 10). Therefore, we assumed that Gab1-SHP2 complex might have the inhibitory effects on myogenic differentiation via activation of ERK1/2. To confirm the inhibitory role of ERK1/2 downstream of Gab1-SHP2 complex, myoblasts overexpressing Gab1^{WT} were treated with or without a MEK1/2 inhibitor, U0126, before inducing myoblasts into myogenic differentiation in the presence of IGF-I. U0126 enhanced IGF-I-induced up-regulation of MHC and myogenin in control myoblasts expressing β-gal (Fig. 9, *A* and *B*). Furthermore, U0126 reversed the inhibitory effect of Gab1^{WT} overexpression on up-regulation of MHC and myogenin (Fig. 9, *A* and *B*). We also confirmed that adenovirus-mediated overexpression of dominant-negative MEK1 (MEK1^{DN}) reversed the inhibitory effect of Gab1^{WT} overexpression on IGF-I-induced myogenic differentiation (Fig. 9, *C* and *D*). These findings suggest that Gab1 inhibits IGF-I-dependent myogenesis through activating MEK1/2-ERK1/2 pathway.

Finally, we examined the effect of adenoviral overexpression of constitutively active MEK1 (MEK1^{CA}). Overexpression of MEK1^{CA} repressed the enhanced myogenic differentiation observed in myoblasts overexpressing Gab1$^{\Delta SHP2}$ (Fig. 10, *A* and *B*). Collectively, interaction of Gab1 with SHP2 negatively regulates IGF-I-dependent myogenic differentiation in C2C12 myoblasts via activation of the MEK1/2-ERK1/2 pathway (Fig. 11).

DISCUSSION

In this study, we investigated the role of Gab1 in skeletal muscle differentiation. To our knowledge, this study demon-